

EXPERIMENTAL DESIGN AND DEVELOPMENT OF A TRANSIENT HOT-WIRE APPARATUS TO MEASURE FLUID THERMAL CONDUCTIVITY

A THESIS SUBMITTED TO THE GRADUATE DIVISION OF THE UNIVERSITY OF
HAWAI'I AT MĀNOA IN PARTIAL FULFILLMENT OF THE REQUIREMENTS FOR THE
DEGREE OF
MASTER OF SCIENCE
IN
MECHANICAL ENGINEERING
May 2022

By

Takuya Paul Wise

Thesis Committee:

Woochul Lee, Chairperson

Joseph J. Brown

Weilin Qu

William E. Uspal

Keywords: Thermal conductivity, heat transfer, transient hot-wire method

©Copyright 2022

by

Takuya P. Wise

All Rights Reserved

ACKNOWLEDGMENTS

First, I am eternally grateful to have worked with Dr. Woochul Lee in the Energy Transport and Conversion Laboratory in the Mechanical Engineering Department at the University of Hawaii at Manoa. His expertise in thermal transport research changed my perspective on heat transfer. This work has been supported in part by Award Number 2034824 from the National Science Foundation.

I do thank Dr. Joseph Brown, Dr. Weilin Qu, and Dr. William Uspal for being a part of my thesis committee.

I would also like to thank my laboratory colleagues in the Energy Transport and Conversion Lab. I do thank Christopher Aguilar for his hard work towards the first developed MATLAB code that started up the project for the THWM. I would like to thank Anh Tuan Nguyen for his assistance and helpful suggestions for this project.

I do thank Mr. Lewis Moore for providing his machine expertise towards the milled copper piece for the physical setup to develop the transient hot-wire apparatus.

Finally, I would also like to thank my family for all their support and love as there were times when I wanted to give up. My parents and brother have been a big support to me as they do want me to challenge myself even when times are rough.

ABSTRACT

The thermal conductivity of heat transfer fluids (HTF) is a critical parameter to determine the overall heat transfer of thermal energy storage systems. With the idea to enhance heat transfer of HTFs, measuring thermal conductivity is vital. With different approaches to measure thermal conductivity, the transient hot-wire method (THWM) was the selected technique due to eliminating convection to extract accurate thermal conductivity values of measured fluids. As the THWM has a fully defined theory of extracting thermal conductivity, this thesis aims to illustrate the design and implementation of the custom-designed apparatus. Material procurement and special techniques to utilize a 25 μm diameter platinum wire was possible to develop a THW test bench. Air, isopropyl alcohol (IPA), ethanol, and DI water were tested as base fluids. Experimental results show that the percent error of detecting their thermal conductivities ranged from 0.117-4.772% in experimental error compared to literature values. The overall thesis shows that the developed THW apparatus can determine thermal conductivity values from 0.026 W/mK to 0.73 W/mK for fluids. With the THW test cell capable to detect the thermal conductivity of liquids and gases, this opens to measuring other liquid solutions that are known for their enhanced thermal conductivity values via nanofluids.

Table of contents

| | |
|---|------|
| ACKNOWLEDGMENTS | iii |
| ABSTRACT..... | iv |
| List of tables..... | vii |
| List of figures..... | viii |
| Nomenclature | ix |
| List of abbreviations..... | xi |
| List of Greek letters..... | xii |
| Chapter 1. Introduction..... | 1 |
| 1.1. Introduction | 1 |
| 1.2. Background on solar water heater project | 2 |
| 1.2.1 Direct solar water heater system | 2 |
| 1.2.2 Indirect solar water heater system..... | 3 |
| Chapter 2. Background on nanofluids, thermal transport modes and thermal conductivity measurement techniques..... | 5 |
| 2.1. Background on nanofluids..... | 5 |
| 2.2. Convection..... | 7 |
| 2.3. Thermal conduction..... | 8 |
| 2.4. Literature works on developed thermal conductivity techniques..... | 10 |
| 2.4.1 Guarded hot plate (GHP) method | 10 |
| 2.4.2 Laser flash method (LFM)..... | 12 |
| 2.4.3 Transient plane source (TPS)..... | 13 |
| 2.4.4 Transient hot-wire method (THWM)..... | 15 |
| 2.5. Technique Selection | 16 |
| 2.6. Research objectives | 17 |
| Chapter 3. THW derivation and theory..... | 18 |
| 3.1. Derivation of the THWM..... | 18 |
| 3.2. Utilizing the THW model..... | 22 |
| 3.3. Change in voltage to change in temperature | 23 |
| 3.4. Thermal penetration depth (TPD) | 24 |
| Chapter 4. Designing the transient hot-wire apparatus | 26 |
| 4.1. Platinum wire..... | 26 |
| 4.1.1 Selected material for resistor..... | 26 |
| 4.1.2 Selection of platinum wire size | 27 |
| 4.2. Copper apparatus | 28 |
| 4.3. Electronic systems for THW apparatus | 30 |
| 4.4. Copper leads..... | 32 |
| 4.5. Configuring platinum wire | 33 |

| | |
|---|----|
| 4.5.1 Insulation test | 36 |
| 4.6. Apparatus setup | 37 |
| Chapter 5. Temperature coefficient of resistance of platinum wire | 39 |
| 5.1. Overall setup of TCR measurement | 39 |
| 5.2. Obtained TCR of 50AWG platinum wire | 40 |
| Chapter 6. Transient hot-wire method results | 43 |
| 6.1. Experimental approach for THW apparatus | 43 |
| 6.2. Preparing THW apparatus before testing | 45 |
| 6.3. THWM for air | 46 |
| 6.4. THWM for isopropyl alcohol | 50 |
| 6.5. THWM for ethanol | 52 |
| 6.6. THWM for deionized (DI) water | 55 |
| 6.7. Validation of the analyzed data | 57 |
| 6.8. Discussion | 59 |
| Chapter 7. Conclusion and Future Works | 61 |
| 7.1. Conclusion | 61 |
| 7.2. Future Works | 62 |
| References | 64 |
| Appendices | 68 |
| Appendix A: Thermophysical properties of conventional fluids | 68 |
| Appendix B: MATLAB Codes utilized | 73 |
| B.1 Raw data extraction data (from THW setup) | 73 |
| B.2 Averaging extracted data MATLAB code | 74 |
| B.3 Code to initiate thermal conductivity measurement | 75 |

List of tables

| | |
|--|----|
| Table 6.1. Experimental trials from THWM measuring air at 22°C vs referenced value | 49 |
| Table 6.2. Experimental trials from THWM measuring IPA at 22°C vs referenced value | 51 |
| Table 6.3. Experimental trials from THWM measuring ethanol at 22°C vs referenced value | 54 |
| Table 6.4. Experimental trials from THWM measuring DI water at 22°C vs referenced value .. | 57 |
| Table 6.5. Measured thermal conductivity of fluids vs referenced values at 22°C | 60 |
| Table A.1. Water's thermophysical properties at atmospheric pressure [6] | 68 |
| Table A.2. Thermophysical properties of air at atmospheric pressure [6]..... | 69 |
| Table A.3. Thermophysical properties of ethylene glycol at atmospheric pressure [6] | 70 |
| Table A.4. Ethanol's thermal conductivity at different temperatures [48] | 71 |
| Table A.5 Isopropyl alcohol's thermal conductivity at different temperatures [47] | 72 |

List of figures

| | |
|---|----|
| Figure 1.1. Direct SWHS: (a.) overall schematic, (b.) electrical heater integrated to the stored water tank..... | 2 |
| Figure 1.2. Annual solar radiation obtained at UHM, data obtained from [4] | 3 |
| Figure 1.3. Indirect SWHS layout..... | 4 |
| Figure 2.1. Alumina nanofluids with different volume fractions of suspended nanoparticles [8] . | 5 |
| Figure 2.2. Nanofluid preparation with the two-step method [11]..... | 6 |
| Figure 2.3. Forced convection over a solid surface [6]..... | 7 |
| Figure 2.4. Thermal conductivity of bulk materials: (a) solids, (b) liquids, (c) gases [6] | 9 |
| Figure 2.5. Guarded hot plate: a. physical setup, b. schematic of setup [15] | 12 |
| Figure 2.6. Schematic of the LFM [18] | 13 |
| Figure 2.7. Overall setup of the TPS: (a) heat diffusing to the sample from TPS sensor, (b) sandwiching two identical materials between TPS sensor [22]..... | 14 |
| Figure 2.8. THWM setup with data analyzed to measure base fluids of deionized water (DI water) and ethylene glycol [30] | 16 |
| Figure 3.1 Diagram of the wire's temperature rise of the natural logarithmic time at a fixed point in the fluid [35] | 21 |
| Figure 3.2. Temperature vs $\ln(t)$ graph for the THWM [39] | 23 |
| Figure 3.3 TPD accommodation: (a.) data extraction from literature utilizing time duration of TPD [28], (b.) cavity width and radial distance for heat to diffuse from the wire and wall to fulfill the THWM..... | 25 |
| Figure 4.1. Plotted wire diameters corresponding to AWG with a close-up view of 50AWG. Data from [42] | 26 |
| Figure 4.2. SolidWorks drawing of designed copper apparatus | 29 |
| Figure 4.3. SolidWorks drawing of designed copper apparatus cover | 30 |
| Figure 4.4. Plotted wire diameters corresponding to AWG with a close-up view of 30 AWG. Data from [42]..... | 32 |
| Figure 4.5. Illustration to remove platinum wire's insulation | 34 |
| Figure 4.6. Top view of soldering technique within copper cavity | 35 |
| Figure 4.7. Two-probe technique after soldering platinum wire | 36 |
| Figure 4.8. Two-probe technique where the positive lead connected to copper wire and negative lead dipped in liquid..... | 37 |
| Figure 4.9. Developed transient hot-wire setup | 38 |
| Figure 5.1. TCR setup: (a.) thermocouple data logger, (b.) DMM, (c.) voltage amplifier, (d.) current source, (e.) copper apparatus with water | 40 |
| Figure 5.2. Platinum wire's temperature coefficient of resistance | 41 |
| Figure 6.1. Front cross-sectional view of the designed copper cavity to reference radial distance for TPD. | 46 |
| Figure 6.2. Data obtained from THW apparatus for measuring air | 48 |
| Figure 6.3. Data obtained from THW apparatus for measuring IPA | 52 |
| Figure 6.4 Data obtained from THW apparatus for measuring ethanol | 55 |
| Figure 6.5. Data obtained from THW apparatus for measuring DI water | 56 |
| Figure 6.6. complied data with air, IPA, ethanol, and DI water | 58 |
| Figure 6.7. Close up view of the complied data of IPA, ethanol, and DI water..... | 59 |

Nomenclature

| | |
|--------------------|---|
| A | Cross-sectional area (m^2) |
| A_s | Surface area (m^2) |
| C | Volumetric heat capacity ($\text{J}/\text{m}^3 \text{K}$) |
| c_p | Isobaric specific heat capacity (J/kgK) |
| $^{\circ}\text{C}$ | Degrees Celsius |
| h | Heat transfer coefficient ($\text{W}/\text{m}^2 \text{K}$) |
| I | Current (mA) |
| k | Thermal conductivity (W/mK) |
| K | Kelvin |
| k_f | Thermal conductivity of the fluid (W/mK) |
| L | Length (m) |
| L_C | Characteristic length (m) |
| L_{TPD} | Thermal penetration depth (m) |
| N | Number of trials |
| Nu | Nusselt number |
| q | Heat transfer rate (W) |
| q' | Heat generated per unit length (W/m) |
| q'' | Heat flux (W/m^2) |
| r | Radial distance (m) |
| R | Resistance (Ω) |
| R_{ref} | Referenced resistance (Ω) |
| $slope_{TCR}$ | TCR slope (Ω/K) |

| | |
|---|--|
| t | time (s) |
| t_1 | Referenced time (s) |
| t_2 | Final time (s) |
| T_{ref} | Referenced temperature (K) |
| x, y, z | Distance (m) |
| \bar{x} | Average value of all conducted trials |
| ∇T | Temperature gradient operator (K) |
| ΔR | Change in resistance (Ω) |
| ΔT | Change in temperature (K) |
| ΔV | Change in voltage (V) |
| $\frac{\partial T}{\partial x}, \frac{\partial T}{\partial y}, \frac{\partial T}{\partial z}$ | temperature gradient with respect to x, y, and z direction |

List of abbreviations

| | |
|------|---------------------------------------|
| AWG | American Wire Gauge |
| DAQ | Data Acquisition |
| DI | Deionized |
| DMM | Digital Multimeter |
| HTF | Heat Transfer Fluids |
| IPA | Isopropyl Alcohol |
| LFM | Laser Flash Method |
| PTFE | Polytetrafluoroethylene |
| SWHS | Solar Water Heater System |
| TCR | Temperature Coefficient of Resistance |
| THW | Transient Hot-Wire |
| THWM | Transient Hot-Wire Method |
| TPD | Thermal Penetration Depth |
| TPS | Transient Plane Source |
| UHM | University of Hawaii at Manoa |

List of Greek letters

| | |
|----------------|---|
| α | Thermal Diffusivity (m^2/s) |
| α_{TCR} | Temperature Coefficient of Resistance (K^{-1}) |
| γ | Euler Constant |
| ρ | Density (kg/m^3) |
| ρ_{res} | Electrical Resistivity ($\Omega \cdot \text{m}$) |
| σ | Standard Deviation |
| σ_{SEM} | Standard Error of Mean |
| μm | Microns |

Chapter 1. Introduction

1.1. Introduction

Heat transfer fluids (HTF) of a solar water heater system (SWHS) has been the lack of attention towards thermal transport as researchers focus on the enhancement of solid materials to enhance heat transfer. Convective HTF such as water and ethylene glycol are commonly used for heating and/or cooling purposes [1]. With water known for its high specific heat capacity, thermal energy can transfer without raising the temperature of the liquid too quickly compared to ethylene glycol (shown in Appendix A table A.1 and, table A.3). Ethylene glycol is well known for having a lower freezing and higher boiling temperature range compared to water [1]. However, water and ethylene glycol tend to have low thermal conductivity values which dictates how much heat can transfer through pure conduction (thermal conductivity values are shown from appendix A table A.1 and table A.3).

The aim of this thesis is to touch upon the continuing work of enhancing a SWHS towards Hawaii's climates. With the possibility to enhance the HTF of the SWHS, it is crucial to know that convection and thermal conduction are the main modes of heat transfer for the stored water tank to reach its optimal hot temperature. To enhance heat transfer, thermal conduction must increase. However, to determine fluids thermal conductivity, measuring this thermophysical property must be investigated to determine if it is conductive or an insulative substance. With Hawaii plan to transitioning towards the renewable energy route by the year 2045 [2], accomplishing the enhancement of the SWHS may result in a promising future towards energy conversion.

1.2. Background on solar water heater project

1.2.1 Direct solar water heater system

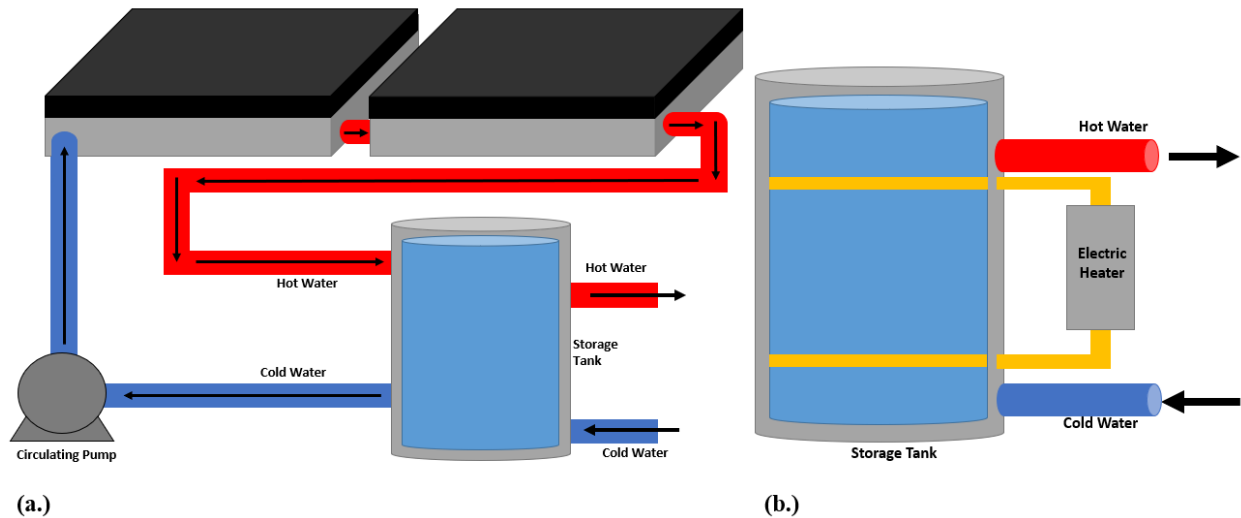


Figure 1.1. Direct SWHS: (a.) overall schematic, (b.) electrical heater integrated to the stored water tank

With SWHS used for commercial and household purposes, an auxiliary electrical heater is typically used [3]. A direct SWHS utilizes this electrical system during cold seasons shown in figure 1.1. This will ensure that the temperature of the stored water tank is able to rise to its optimal hot temperature range of 140°F [3]. With the use of an electrical heater, electricity converts to heat and is transferred to the water tank from joule heating. This process becomes more costly with utilizing too much electricity for even household residents or businesses and water itself has a relatively high specific heat capacity. However, solar radiation during the summer season is high [4] and can be used for energy conversion especially for direct and/or indirect SWHS. Figure 1.2 contains the annual solar radiation in Hawaii [4] to illustrate that the summer sessions extracts more solar radiation than any other seasons of the year (May to August).

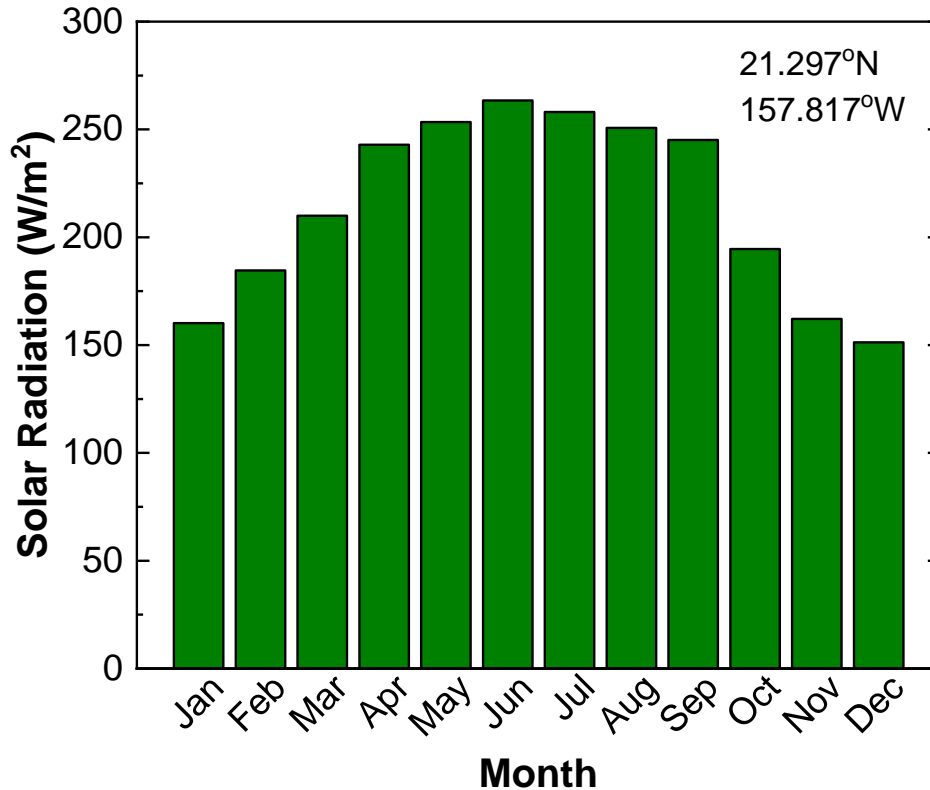


Figure 1.2. Annual solar radiation obtained at UHM, data obtained from [4]

1.2.2 Indirect solar water heater system

Next up is an indirect SWHS. Figure 1.3 illustrates an indirect SWHS that utilizes an antifreeze solution (such as water/ethylene glycol mixed solutions) to extract the necessary thermal energy from the solar absorbers to the stored water tank without any physical mixing [3]. The entire setup of an indirect SWHS can be viewed as a large heat exchanger, which divides into two closed loops. One loop containing the HTF and the other loop with the stored water that will be used for . The principle behind the indirect SWHS is that the HTF extracts the heat from the solar absorbers and flows to the stored water tank. The entire piping system is thermally insulated to allow all the heat to transfer into the storage tank over time. Once the hot HTF passes through the copper coil within the storage tank, the working fluid is at a lower

temperature since heat was transferred to the water tank. The HTF continuously flows in the same loop until the stored water tank reaches to its optimal hot temperature range. The water tank within the SWHS also relies on natural convection as heat is transferred from the density and temperature differences that drives recirculating fluid motion [5, 6]. With the idea to enhance the working fluids in a SWHS, the use of nanofluids would allow the overall heat transfer of the water tank to reach its optimal temperature range of 140°F [3] quicker compared to conventional HTF such as water and/or ethylene glycol.

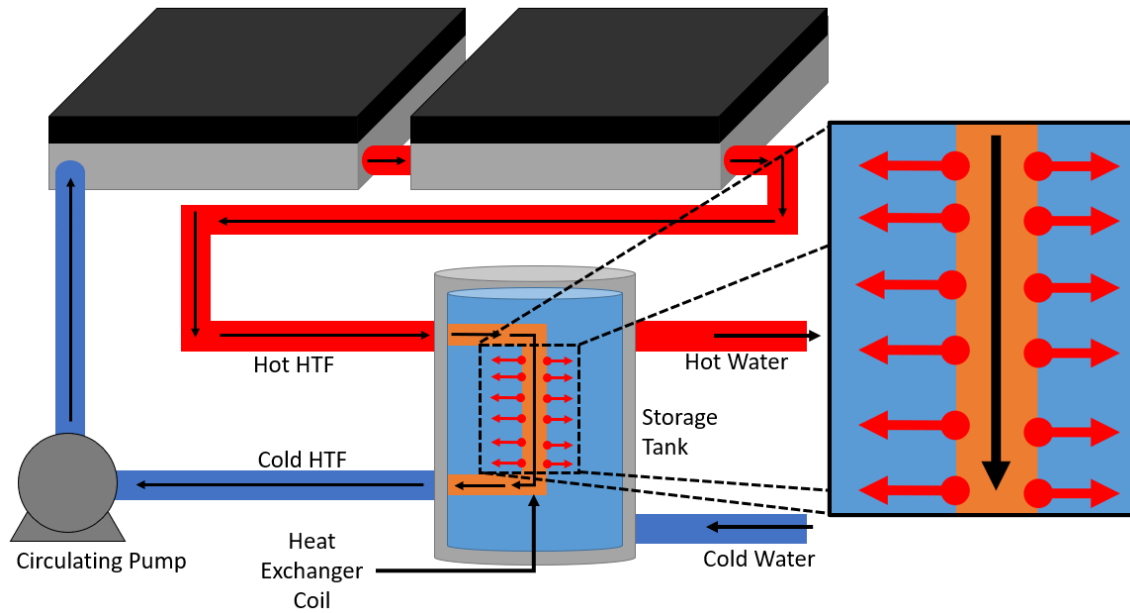


Figure 1.3. Indirect SWHS layout

With the idea to enhance the HTF of a SWHS, nanofluids was the selected candidate towards this work due to their well-known ability towards their enhanced thermal conductivity values compared to their base liquids [7].

Chapter 2. Background on nanofluids, thermal transport modes and thermal conductivity measurement techniques

This chapter will introduce the background on nanofluids, the two main modes of heat transfer for fluids which are convection and thermal conduction. This chapter will also include literature works of different thermal conductivity measurement techniques to distinguish what type of approach shall be done to design and implement for this thesis work.

2.1. Background on nanofluids

Nanofluids are colloidal solutions well known for their enhanced thermal conductivity values comparing to their base liquids such as water, ethylene glycol, etc. Nanofluids contains nanoparticles from the size of 1-100nm [7]. A few materials used for nanofluids consists of silver, alumina, diamond, carbon nanotubes, etc. as the solid particles [7]. Figure 2.1 illustrates a physical preparation of alumina nanofluids with different volume fractions of the suspended nanoparticles [8].

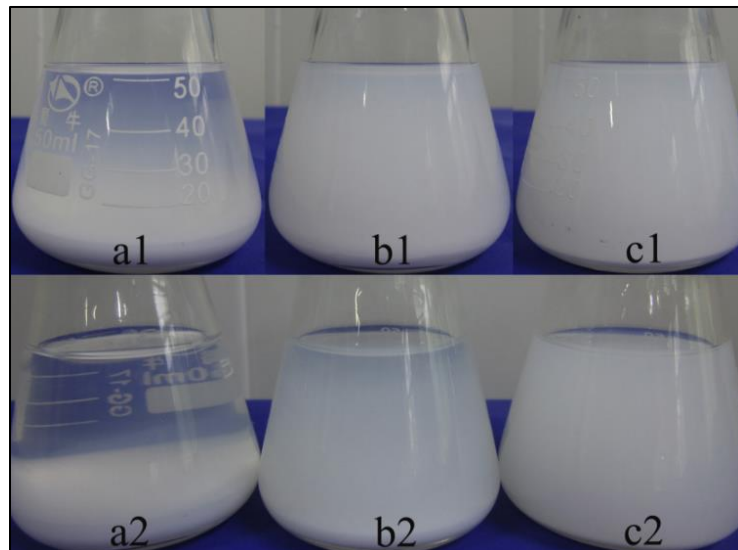


Figure 2.1. Alumina nanofluids with different volume fractions of suspended nanoparticles [8]

With nanofluids as the hot topic towards thermal engineering, researchers do need to investigate an optimal approach of how to enhance base liquid's thermal conductivity with the number of nanoparticles and surfactants to ensure that the colloids are stabilized to enhance the heat transfer of the fluid. It has been said that nanofluids enhance the overall heat transfer of the base fluid due to the present of nanoparticles. The nanoparticle's surface to volume ratio is significantly higher than microparticles, which allows the heat to conduct onto the nanoparticles' surface area to the liquid's interface [9]. For the nanoparticles to stabilize within the medium, surfactants (or surface-active agents) are used to reduce the surface tension of the liquid. The common technique is the two-step method [10, 11] in which the nanoparticles are measured out and dispensed into the base liquid. This is followed up with an ultrasonic process to distribute the surfactants and nanoparticles within the medium for a uniform mixture as shown in figure 2.2 [11].

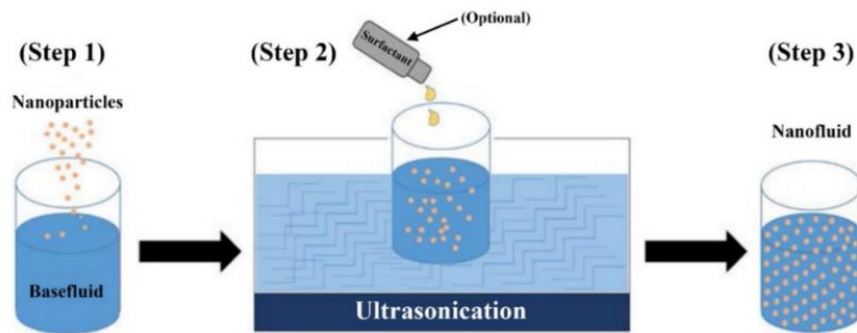


Figure 2.2. Nanofluid preparation with the two-step method [11]

As the work towards nanofluids are in development towards the stabilization and heat transfer enhancement, the overall idea behind these suggested colloidal solutions is the fact that they exhibit thermal conductivity enhancement that can be utilized for energy conversion. This brings into the next section as thermal convection and conduction are the modes of thermal transport that helps govern the ability of fluids to transfer heat.

2.2. Convection

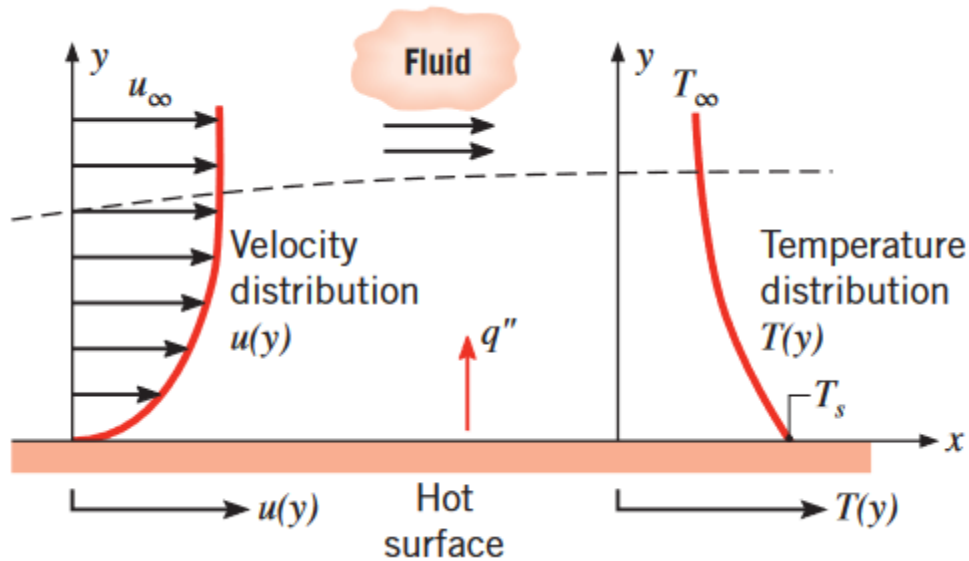


Figure 2.3. Forced convection over a solid surface [6]

First up, thermal convection is the major mode of heat transfer towards fluids. The two types of convections are natural and forced [5]. Natural convection is reliant to buoyancy forces due to density differences of hot and cold fluids while forced convection is where the liquid or gas is in motion along the solid surface that is either hot or cold [5, 6]. From figure 2.3, the no-slip boundary illustrates that heat is only transferred by thermal conduction which is also backed up by the claim that conduction allows heat to flow from hot to cold regions without any bulk or macroscopic motion [6]. Convection is governed after the no-slip boundary due to two boundary layers (velocity and thermal) [6]. This is related when there is a temperature gradient between the solid surface and bulk fluid [5]. Convection heat transfer is also obtained from Newton's Law of cooling shown in equation 2.1:

$$q = hA_s \Delta T \quad (2.1)$$

The q , h , A_s , and ΔT , represents the convection heat transfer rate, heat transfer coefficient, surface area, and the change in temperature, respectively [6]. The heat transfer coefficient is not a thermophysical property of a specific material, it is a flow property that is governed by the type of fluid properties, flow field, and the geometry of the solid surface that the liquid or gas flows over [5]. From equation 2.1 (Newton's Law of cooling) it shows that q is proportional to h , A_s , and ΔT . This means that to enhance the overall heat transfer rate for the HTF from thermal convection, the thermal conductivity would have to increase as this utilizes the Nusselt number. The Nusselt number is the ratio of convection heat transfer to thermal conduction of the fluid across the boundary [6]. The Nusselt number equation is followed:

$$Nu = \frac{hL_c}{k_f} \quad (2.2)$$

Variables Nu , h , L_c , and k_f represents the Nusselt number, convection heat transfer coefficient, characteristic length, and the thermal conductivity of the fluid [6]. Rearranging equation 2.2 to solve for the convection heat transfer coefficient is shown to be:

$$h = \frac{Nuk_f}{L_c} \quad (2.3)$$

From observing equation 2.3, h is proportional to the Nu and k_f which shows that if k_f increase, then the convection heat transfer coefficient increases too which allows the fluid of interest to transport heat from the solid surface or vice versa.

2.3. Thermal conduction

Thermal conduction is the main transport mechanism that measures how heat is transferred from different materials/substances. As mentioned before, thermal conduction occurs when heat is transferred from hot to cold when there is no bulk or macroscopic motion of the

material/substance. The governing equation to measure conduction heat transfer is from Fourier's law:

$$q'' = -k\nabla T \quad (2.4)$$

The q'' , k , and ∇T are the local heat flux, thermal conductivity of the material, and the gradient operator of the change in temperature [5]. The ∇T , helps to determine the direction for a 3-dimensional analysis of thermal conduction which is governed by:

$$\nabla T = \frac{\partial T}{\partial x} \hat{x} + \frac{\partial T}{\partial y} \hat{y} + \frac{\partial T}{\partial z} \hat{z} \quad (2.5)$$

The variables $\frac{\partial T}{\partial x}$, $\frac{\partial T}{\partial y}$, and $\frac{\partial T}{\partial z}$ represents the temperature gradient corresponding in the x, y, and z direction, respectively. As this is only with respect to Cartesian coordinates, equation 2.5 can also be utilized for cylindrical and/or spherical coordinates. The main parameter that drives Fourier's law equation for heat transfer is thermal conductivity as many bulk materials are unique towards the ability to insulate or conduct thermal energy.

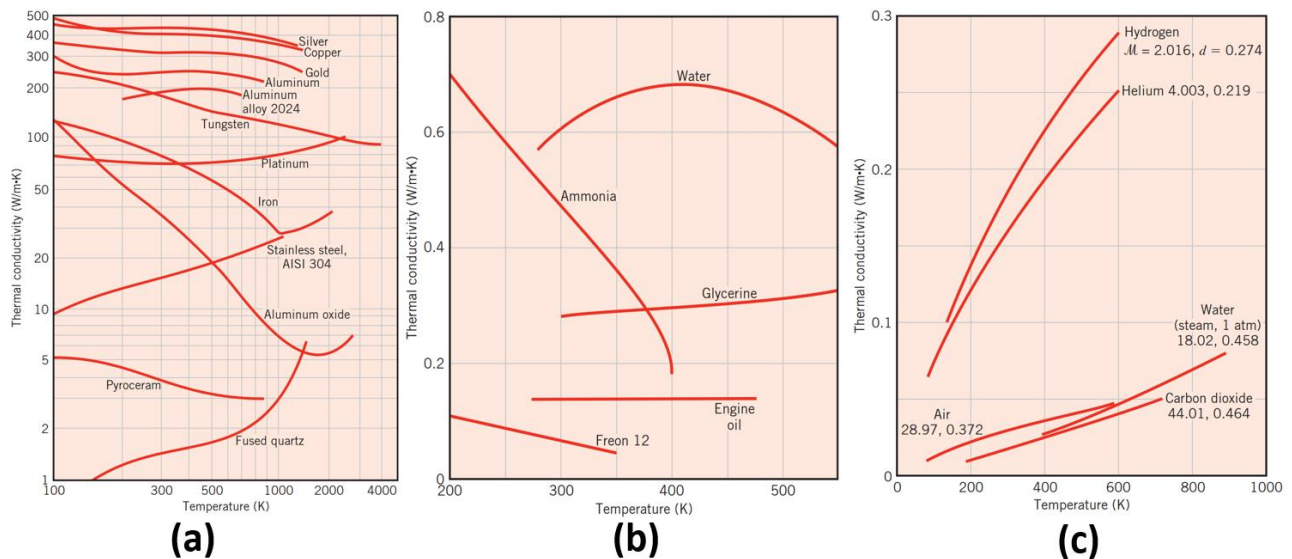


Figure 2.4. Thermal conductivity of bulk materials: (a) solids, (b) liquids, (c) gases [6]

Thermal conductivity is a vital thermophysical property to indicate if materials or substances are either insulators or conductors [6]. Thermal conductivity of bulk materials are referenced from reliable literatures/academic textbooks that have been experimentally measured as shown in figure 2.4 for solids, liquids, and gases. However, as materials (especially nanomaterials or powders) and liquid substances are altered, thermal conductivity cannot be referenced as there is no publications on their thermophysical properties. In other words, when fluids or materials are experimentally designed or altered from laboratory procedures, properties such as mechanical, electrical, and thermophysical properties can change. This shows that experimentation is vital to measure thermal conductivity of unknown materials/substances via nanofluids.

2.4. Literature works on developed thermal conductivity techniques

With the idea to measure thermal conductivity towards new synthesized substances, it is vital to select a suitable technique that does provide consistent results. This breaks into two categories which are accuracy and precision. The goal of any experiment is to extract accurate results that is able to result to the closeness of the expected value [12]. Precision is another key factor that indicates that each repeated trial are consistent with each other that is also related to the standard deviation [12]. Having a low standard deviation provides the user that the extracted experimental results do have a low spread and are in range of the extracted data. The listed techniques in this section will provide a foundation of how each system works and their fundamental principle of how measurements are taken for either fluid or solids.

2.4.1 Guarded hot plate (GHP) method

First off, the guarded hot plate (GHP) is the common approach for measuring bulk solid materials [13]. The bulk solid sample is sandwiched between a hot and cold plate. This approach

relies on the steady state temperature which dictates that the system must be at thermal equilibrium to extract the material's thermal conductivity. Using Fourier's law of heat conduction in 1-direction [6] is calculated to obtain thermal conductivity of the bulk material.

This equation is shown to be:

$$q = -kA\left(\frac{\partial T}{\partial x}\right) \quad (2.6)$$

The variables q , k , A , ∂T , and ∂x represents the heat transfer rate from thermal conduction, thermal conductivity of the material, cross-sectional area in which heat is transferred, the change in temperature, and the distance that the heat is transferred, respectively. The negative sign helps to distinguish which direction heat is flowing since heat transfers from hot to cold regions along the material. To solve for k , equation 2.6 must be rearranged in which results to:

$$k = -\frac{q}{A}\left(\frac{\partial x}{\partial T}\right) \quad (2.7)$$

For the GHP method to work with Fourier's law, the cold and hot plate must have a consistent temperature that does not change as the material of interest also comes into thermal equilibrium. This is to show that a long-time duration must be implemented for the temperature of the two plates and materials cannot change for a long duration. Insulation is also used to ensure that the bulk material does not lose heat from convection during the experiment. The main drawback of this specific technique is the capability to measure fluid's thermal conductivity [14]. Figure 2.5 illustrates the overall setup of the hot guarded plate technique which utilizes a solid bulk material during the experiment.

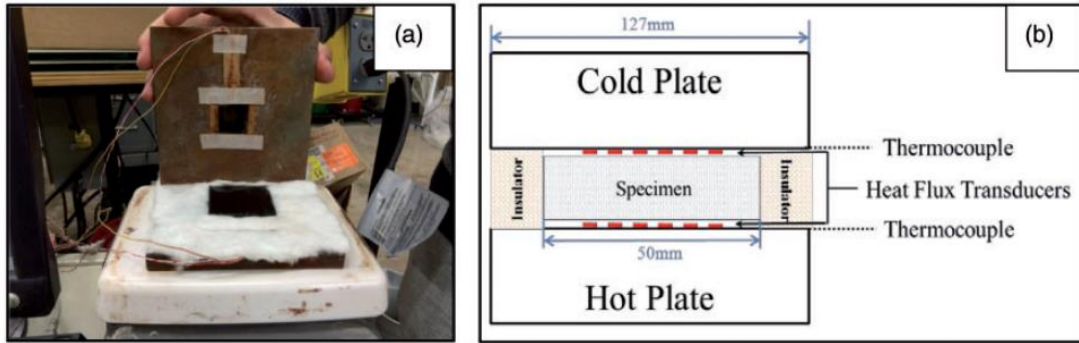


Figure 2.5. Guarded hot plate: a. physical setup, b. schematic of setup [15]

2.4.2 Laser flash method (LFM)

Next, the laser flash method (LFM) is an unsteady state technique that utilizes a laser pulse that allows the heat to propagate through a material [3, 5]. This technique mainly measures thermal diffusivity to extract thermal conductivity [16]. Parker was the first scientist to develop this technique in order to measure thermal diffusivity of solid materials only from the temperature ranges of 22°C and 135°C [17]. The bulk material usually requires a specific shape that can be placed under the apparatus. The sample that is tested with the LFM is coated with a material such as graphite to emit and absorb the laser pulse during the experiment [13]. A radiation thermometer is used to monitor the temperature of the sample over a short period of time to extract thermal diffusivity and other thermophysical properties. The data is analyzed by taking half of the overall temperature rise with the corresponding time duration the experiment took from the transient temperature profile from the LFM [10, 11]. Figure 2.6 illustrates the physical setup of the LFM.

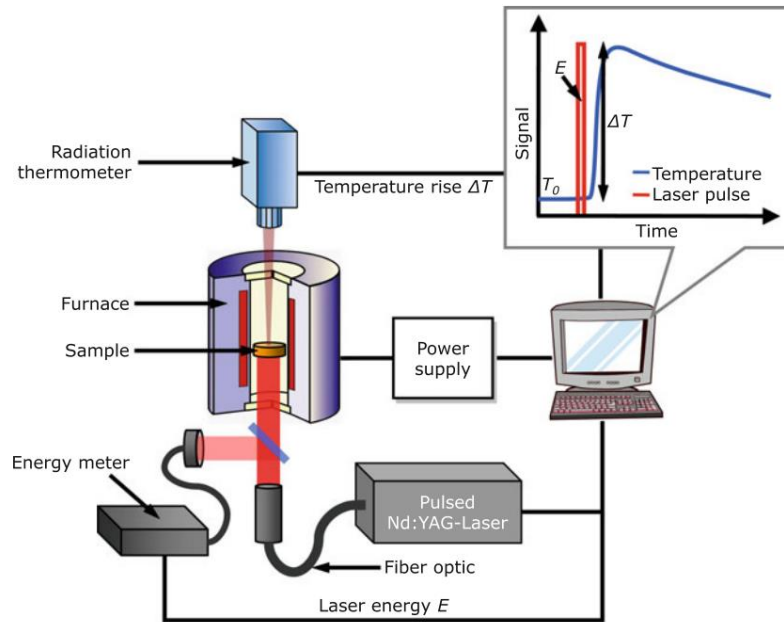


Figure 2.6. Schematic of the LFM [18]

According to Tada, it is possible to measure liquid's thermal conductivity with the LFM [19] however, the heat flux passing through the container cannot be neglected during the experiment [20]. This illustrates that during the LFM test, the extracted data will include the temperature rise of the container and fluid of interest to analyze the thermal diffusivity and thermal conductivity. Another thing is that the LFM requires an input of the material's density and specific heat capacity [20] to obtain thermal diffusivity and thermal conductivity. The LFM test bench also needs to be tested in a vacuum to prevent any convection heat loss during the experimentation [17]. All in all, the LFM is beneficial towards solid materials that can also be electrically conductive at high temperatures [17].

2.4.3 Transient plane source (TPS)

The transient plane source (TPS) is another unsteady state technique also known as the "hot disk" technique [21]. This method is aimed to measure material's thermal conductivity ranging from liquids, pastes, and solids without the present of natural convection from the

selected time range for the temperature profile plot for the TPS technique. The TPS acts as a heat source and a resistance thermometer to detect the temperature response of the sensor over time [21]. This is based off the joule heating effect as current passes through the conductive coil but does not allow the current to leak into the material (even if it is a conductive material) as there is a uniform layer of Kapton around the TPS sensor. With the heat transferred to the material (illustrated in figure 2.7a), the sensor's temperature response will dictate if the material is an insulator or conductor. The TPS method requires the sensor to be sandwiched between two identical materials (shown in figure 2.7b) to initiate the transient technique [15, 16]. With a high temperature response from the sensor, it will show that the material is an insulator while a low temperature response will indicate that a conductive material has been measured.

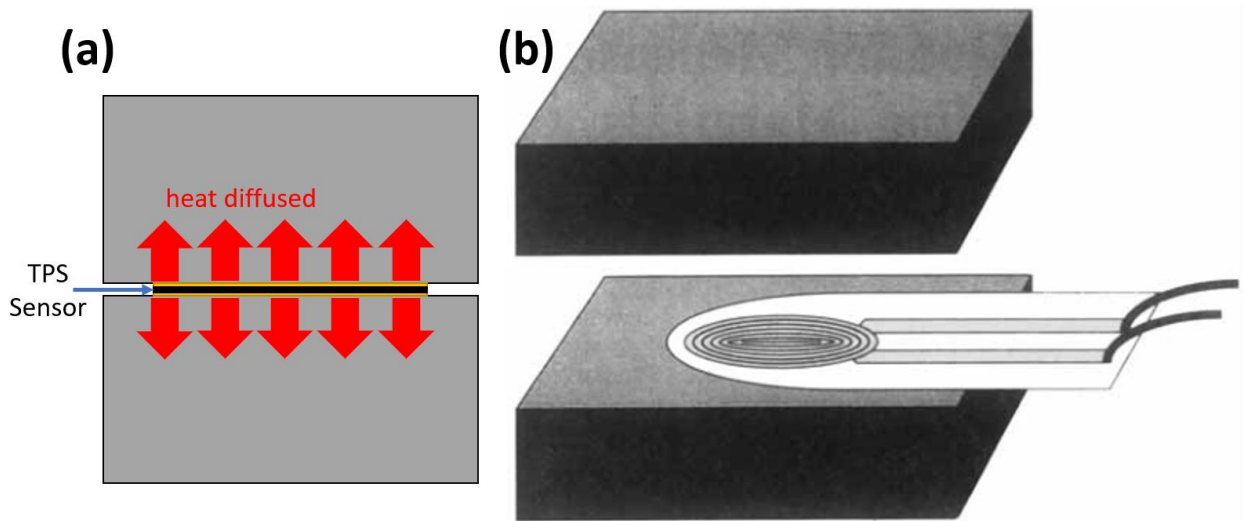


Figure 2.7. Overall setup of the TPS: (a) heat diffusing to the sample from TPS sensor, (b) sandwiching two identical materials between TPS sensor [22]

The downside towards the TPS method is that the sample being measured must have a specific dimension to accommodate the thermal penetration depth (TDP). TDP is the distance in which heat is diffused through a material over time [23]. This is an important parameter because

this indicates that the sensor's signal is influenced by another factor other than the measured substance. Another downside to this technique is that the insulation of the sensor may affect the time range to extract thermal conductivity from the temperature profile plot. In other words, the sensor has its own heat capacity which influences the heat transfer between the measurement instrument and the material of interest [24]. Even from the joule heating effect within the coil, the sensor's insulation will also be present within the temperature response. Overall, the TPS technique does require the TPD to not exceed the material's thickness and heavily rely on the use of adjusting the time range to accommodate the insulation material as the temperature response of the sensor is detecting thermal conductivity of the desired substance.

2.4.4 Transient hot-wire method (THWM)

Lastly, the transient hot-wire method (THWM) is a popular technique which utilizes a very thin wire as the main resistor [8, 9]. This approach is modeled as a line source where the wire is infinitely thin [26] meaning that the wire changes temperature from the applied step voltage. This also illustrates that the thin wire dissipates a uniform heat flux [25] around the surface area in contact with the material of interest. The dissipated heat from the thin wire only transfers to the material by thermal conduction. Convection is eliminated during the data analysis process as it occurs at later time durations [15, 18]. The joule heating effect from the wire also contributes to the change in temperature of the wire due to the change in resistance (temperature coefficient of resistance (TCR) is further discussed in section 5.2). Published literature towards utilizing the THW technique has been shown that the test cell is a reproducible system to calibrate and measure thermal conductivity of substances/materials [11–15]. Literature works utilize a Wheatstone bridge to extract the small voltage drops of the resistor in contact with the substance of interest [8, 9, 14, 16]. From figure 2.8, the potentiometer is adjusted until the

voltage bridge was balanced in which a current was applied to allow the hot-wire to change in resistance to convert into the change in temperature [30].

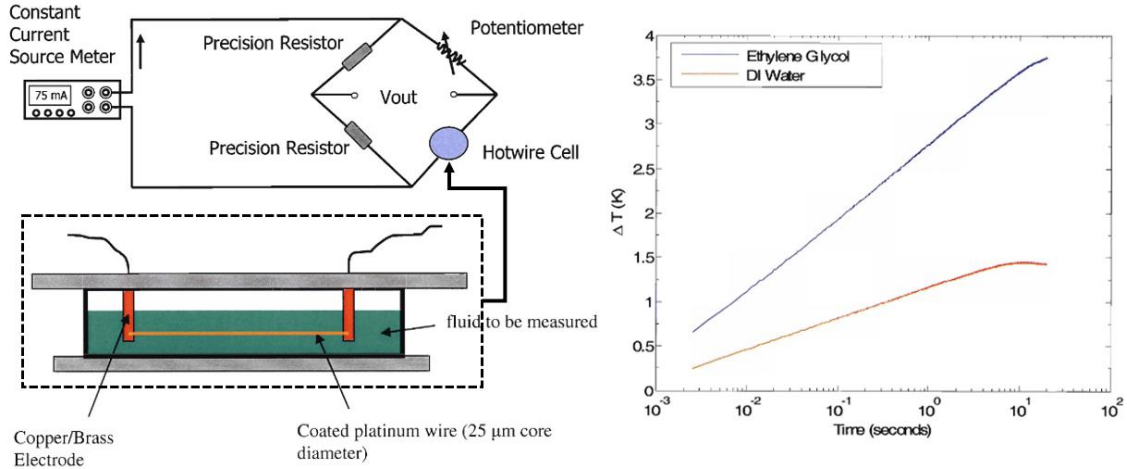


Figure 2.8. THWM setup with data analyzed to measure base fluids of deionized water (DI water) and ethylene glycol [30]

The main drawback of this technique is utilizing a very thin resistor that is fragile during the design process [9]. Even though there are commercialized products specifically with the THWM, many literature works do utilize the idea to design and implement their own THW apparatus as it builds the foundation of how the system operates [18-23]. This shows that the THWM is a reproducible system to measure thermal conductivity of substances. The limitation that the THW test can be utilized is towards fluids as the entire surface area of the wire must be in contact as heat is transferred directly from the surface of the wire to the substance's interface as the no-slip boundary condition exists for thermal conduction.

2.5. Technique Selection

With the four popular techniques reviewed to measure material's thermophysical properties, the THWM was the selected technique. With the goal to measure fluid's thermal conductivity, having the fluid in contact with the thin wire is possible as it only requires having

an apparatus that is an open/closed system. This means that the fluid will be dispensed into a vessel before the experiment (opened) and the cavity will be closed during the experimentation, so liquid does not flow out. Since the measured substances are only liquids, the internal volume of the designed test cell must be constant to ensure a consistent amount of material is measured in the designed THW test cell. With the THWM eliminating thermal convection [15, 21, 24], this approach was the selected technique to design and implement towards this thesis work as it eliminates any misleading results towards measuring thermal conductivity of known fluids and nanofluids.

2.6. Research objectives

The goal of this thesis work is to design and develop a THW apparatus that can accurately detect thermal conductivity of different fluids. To achieve the goal, literature works were reviewed to investigate an optimal approach to construct and develop a THW test cell for fluids along with developing a MATLAB code to initiate the experimental apparatus to obtain thermal conductivity of liquids and gases. This will indicate that known thermal conductivity values for air and water is traceable from utilizing the developed THW apparatus. The custom-designed test cell shall be used to measure novel substances/materials such as nanofluids.

Chapter 3. THW derivation and theory

This chapter aims to provide a brief understanding of utilizing the THWM equation for data extraction and analyzing thermal conductivity. The derivation of the THW model will illustrate how thermal conductivity is obtained.

3.1. Derivation of the THWM

Over time, the THWM equation has been fully developed from modeling as an infinite line source [26]. In the past, the THWM was aimed to measure thermal conductivity of different gases which also utilizes temperature correction factors to extract thermal conductivity of the gases due to other effects [13, 14]. For this thesis, the only gas measured is air which did not need to accommodate for any temperature factors. For that, this work utilized no correction factors to help obtain fluids thermal conductivity through the THWM.

Over time, the THWM mathematical model has been fully developed by Nagasaki and Nagashima for an insulated thin wire aimed to measure electrically conductive liquids [32]. Equation 3.1 is derived off the heat equation in cylindrical coordinates with time and the radial distance that the heat is generated from the hot-wire to the substance of interest [36]. The wire must be long enough to neglect any end effects so there is a uniform heat flux generated to the medium over the short time interval [18, 26]. As the THWM mathematical model is based on the wire to generate constant heat from start to finish, the general heat equation to conduct the THWM is shown:

$$\Delta T (r, t) = \Delta T = \frac{q'}{4\pi k} \ln\left(\frac{4\alpha t}{r^2 \gamma}\right) \quad (3.1)$$

The variables of $\Delta T(r, t)$, q' , t , r , γ , k , and α represents that temperature is a function with respect to the radial distance and time, the heat generated per length of the wire, the time

duration, radial distance of the wire, Euler constant ($\gamma = e^{0.5772} = 1.781\dots$), thermal conductivity and thermal diffusivity of the measured substance, respectively. The variable α thermal diffusivity is expressed as:

$$\alpha = \frac{k}{c_p \rho} \quad (3.2)$$

With k known as the thermal conductivity of the substance, c_p and ρ represents the isobaric specific heat capacity and the density of the same substance, respectively. Equation 3.2 determine the ability of a substance to transport heat relative to its ability to contain thermal energy [6]. Substances with large α will quickly respond to changes in their thermal environments while low α will respond slowly around their thermal environments [6]. This variable is important as it is included in the THW heat equation shown in equation 3.1. This also contributes to the thermal penetration depth (TPD) as it will be mentioned heavily in section 3.4.

Equation 3.1, the THW model can be viewed as how temperature of the wire changes over time (without the need to indicate the heat propagated from the thin wire). Since the change in temperature of the wire indicates that heat transfer occurs within the THW test cell, equation 3.1 can be simplified much further. From following the derivation provided by tec-science, the THW heat equation is simplified from equations 3.3 to 3.7 illustrating the final equation of the THWM [38].

$$\Delta T = T(r, t_2) - T(r, t_1) \quad (3.3)$$

The difference in the change in temperature can be viewed by the final temperature minus the initial temperature of the thin wire immersed in the medium. Equation 3.3 follows from equation 3.1 to have time stamp at different durations during the THW test. The change in temperature of

the wire from two different time stamps can be simply expanded from utilizing equation 3.1 to obtain equation 3.5:

$$\Delta T = \frac{q'}{4\pi k} \ln\left(\frac{4\alpha t_2}{r^2 \gamma}\right) - \frac{q'}{4\pi k} \ln\left(\frac{4\alpha t_1}{r^2 \gamma}\right) \quad (3.4)$$

With $\frac{q'}{4\pi k}$ as the common variable within equation 3.4, the function can be rewritten simply as:

$$\Delta T = \frac{q'}{4\pi k} \ln\left(\frac{\frac{4\alpha t_2}{r^2 \gamma}}{\frac{4\alpha t_1}{r^2 \gamma}}\right) \quad (3.5)$$

With similar variables within the natural logarithm the $\frac{4\alpha}{r^2 \gamma}$ from the numerator and denominator can be cancelled out leaving the time stamps of t_2 and t_1 behind as shown:

$$\Delta T = \frac{q'}{4\pi k} \ln\left(\frac{t_2}{t_1}\right) \quad (3.6)$$

Equation 3.7 is the overall heat equation where the temperature of the thin wire is dependent to the time stamps between t_2 and t_1 . To determine the thermal conductivity of the substance of interest, ΔT and k are rearranged which results to:

$$k = \frac{q'}{4\pi \Delta T} \ln\left(\frac{t_2}{t_1}\right) \quad (3.7)$$

The final equation to determine thermal conductivity of the fluid from the THW experiment is shown in equation 3.7. This shows that with constant joule heating from $\frac{q'}{4\pi}$ of the thin wire, the overall slope is determined by the ΔT vs $\ln\left(\frac{t_2}{t_1}\right)$. Figure 3.1 illustrates a general overview of determining the slope to obtain the substance's thermal conductivity while utilizing the derived heat equation from equation 3.7. This indicates that the slope (ΔT vs $\ln\left(\frac{t_2}{t_1}\right)$) is equivalent to the heat generated per unit length of the wire over the fluid's thermal conductivity.

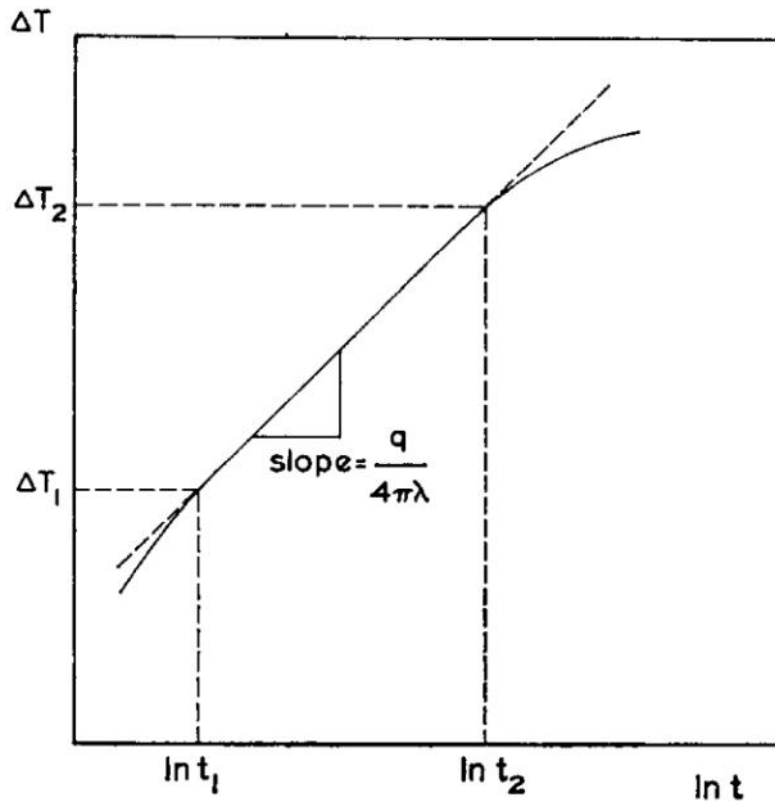


Figure 3.1 Diagram of the wire's temperature rise of the natural logarithmic time at a fixed point in the fluid [35]

At times t_1 and t_2 , a temperature value related to the change in resistance of the wire will be shown. The specific term of t_1 is never the initial point of the THW experiment but sometime later to indicate a constant joule heating effect from the wire to the substance of interest as constant thermal conduction occurs beyond t_2 . After t_2 , the constant joule heating effect may overshoot leading into the convection region during the THW experiment [30], this region does produce an inaccurate reading the material's thermal conductivity as there is no linear region to fit. With the analysis of the temperature response with respect to time of the wire, the plot will show an exponential growth as temperature increases exponentially over time with transient conduction. The exponential plot must be converted to natural logarithmic function of time as it

provides a linear region to fit in the wire's change in temperature with respect to the natural logarithm of time (as shown in figure 3.1).

3.2. Utilizing the THW model

It is been also shown that for the line of best fit to appear on the $\Delta T/\ln(t)$ graph, it relies on the least square method [39]. Figure 3.2 illustrates that the obtained temperature response shows a linear regression between 0.1 to 0.6 seconds [39]. This also illustrates that fitting the line before and/or after the linear range will result an inaccurate measurement in the material's thermal conductivity. Fitting in before the existence of the linear range will result an overestimated thermal conductivity value as the wire is still in the heating phase [40]. The initial wire heating phase does not lead into a constant joule heating effect right away. At some time later, the temperature response over the $\ln(t)$ will show a linear regression indicating the line of best fit region where heat from the wire is transferred to the medium. This specific range happens quickly since the technique is based on transient thermal conduction. To ensure there is consistency of how the data is extracted, it is vital to have a referenced time range to fit in the change in temperature of the wire to measure thermal conductivities of different materials.

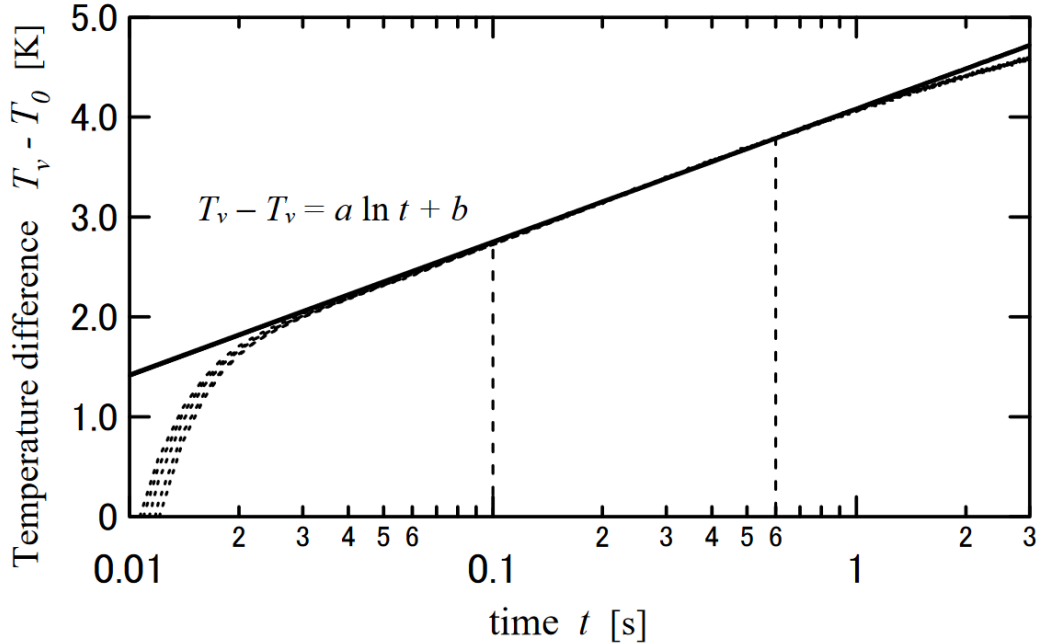


Figure 3.2. Temperature vs $\ln(t)$ graph for the THWM [39]

3.3. Change in voltage to change in temperature

For the THWM, to obtain a change in temperature of the wire, the change in voltage over time must be extracted. To extract a change in voltage, current must pass through a resistor which results in a voltage drop over time. This is related to Ohm's Law which is:

$$\Delta V = I\Delta R \quad (3.8)$$

The variables ΔV , I , and ΔR represents the change in voltage, electrical current, and the change in resistance, respectively. Rearranging equation 3.8 shall provide the following:

$$\Delta R = \frac{\Delta V}{I} \quad (3.9)$$

The variables involved in equation 3.9 are the same from equation 3.8 but shows that the change in resistance equals to the change in voltage divided by the electrical current. With the change in resistance of a thin wire, it can also be expressed with the temperature coefficient of resistance (TCR) equation:

$$\Delta T = \frac{\Delta R}{R_{ref} \alpha_{TCR}} \quad (3.10)$$

Variables of ΔT , ΔR , R_{ref} , and α_{TCR} represents the overall change in temperature, change in electrical resistance, referenced resistance at corresponding temperature, and the wire's temperature coefficient of resistance, respectively. This will help to see how an infinitely thin wire can transfer heat to the surrounding medium.

3.4. Thermal penetration depth (TPD)

Another thing to accommodate in the THWM is the thermal penetration depth (TPD) [6, 18, 31]. TPD is the distance to which significant temperature effects transports within a substance [6]. For the THW test cell, the size and dimensions of the cavity is vital to investigate how quickly heat will propagate within the substance/material. As each material has a different thermophysical properties (more specifically thermal diffusivity α), this dictates how quickly heat is transferred through different substances. TPD can be calculated with:

$$L_{TPD} = \sqrt{4\alpha t} = \sqrt{\frac{4kt}{c_p \rho}} = \sqrt{\frac{4kt}{C}} \quad (3.11)$$

The variables L_{TPD} , t , α , k , c_p , ρ , and C represents the thermal penetration depth, time duration, thermal diffusivity, thermal conductivity, isobaric specific heat capacity, density, and the volumetric heat capacity [28] of the measured material/substance, respectively.

The THWM relies on the heat transfer of the thin wire to the test material by thermal conduction. If the TPD is larger than the cavity's radial distance, then the measurement of the material's thermal conductivity will be incorrect due to the interference of the test section's surface [41]. But if the cavity's distance is larger than the TPD, then the apparatus is capable to detect the selected material's thermal conductivity accurately. Figure 3.3a illustrates that the

obtained data to extract thermal conductivity of DI water and stainless steel 316L from the time range of 0.1 to 0.9 seconds, while 3.3b is the front cross-sectional view of the copper cavity to establish the maximum radial distance to determine TPD. It was also shown that from Wei's work that the largest TPD was approximately 1.1 mm with thermal conductivity, volumetric heat capacity, and time of duration to be 0.8 W/mK, $2.6 \times 10^6 J/m^3 K$, and 0.9 seconds, respectively [28]. This was tolerable because the overall radial distance of the copper cavity was 3.75mm which means that the heat diffused in the material did not propagate more than 3.75mm in less than 1 second but only diffused at 1.1mm which is a shorter radial distance from conducting the THW test.

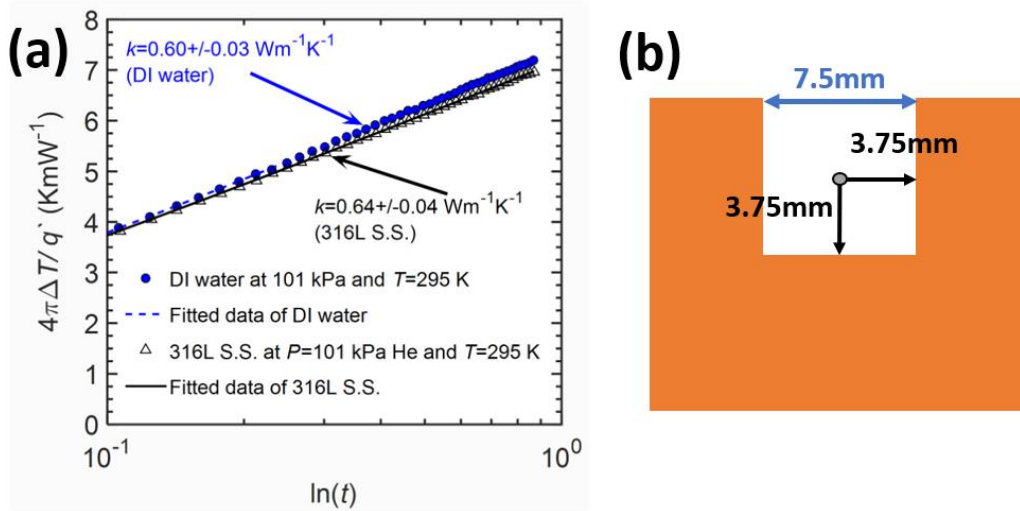


Figure 3.3 TPD accommodation: (a.) data extraction from literature utilizing time duration of TPD [28], (b.) cavity width and radial distance for heat to diffuse from the wire and wall to fulfill the THWM.

Chapter 4. Designing the transient hot-wire apparatus

This chapter will focus on emphasizing what each material or component shall be used for the THW test cell. The techniques to configure the components of the THWM together shall be discussed.

4.1. Platinum wire

4.1.1 Selected material for resistor

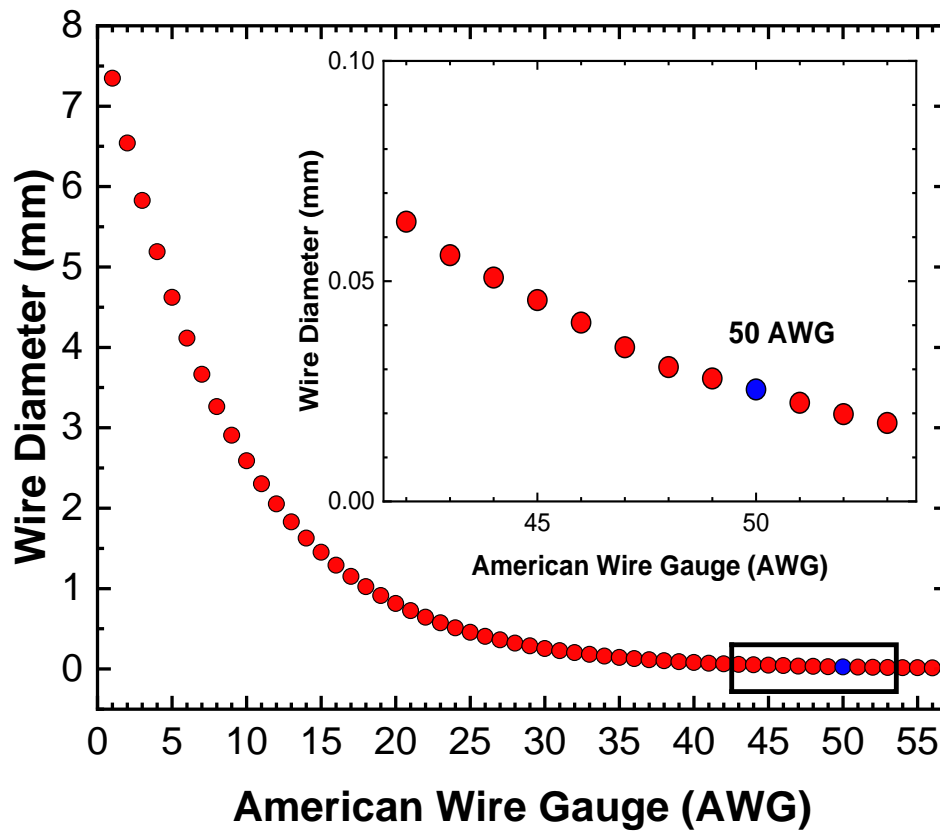


Figure 4.1. Plotted wire diameters corresponding to AWG with a close-up view of 50AWG. Data from [42]

A platinum wire was used as the main resistor for the THWM. The diameter size was also considered as wires do go by specific wire gauges (usually AWG or American Wire Gauge as shown from figure 4.1). AWG sizes plays a role here towards the THW apparatus because to have an optimal resistance of the selected wire, the cross-section must be reduced as it relates towards the electrical resistivity equation:

$$R = \frac{\rho_{res}L}{A} \quad (4.1)$$

The variables R , ρ_{res} , L , and A , represents the wire's nominal resistance, material's electrical resistivity, length of the entire wire, and the cross-section of the wire, respectively. This shows that the cross-section of the wire changes the resistance of the wire significantly as they are inversely proportional to each other.

The platinum wire serves as a very thin heater and a thermometer in the THW apparatus [9]. As platinum is considered as a noble metal, tarnishing is unlikely to happen. Platinum is also a good electrical conductor, indicating that insulation is required for the THW test cell. A 50 AWG isonel-insulated platinum wire (purchased from A-M system) was utilized as the insulating coating was about $1.3\mu\text{m}$ thick and already adhered to the entire platinum wire for 1 spool. The 50 AWG isonel insulated platinum wire makes it a suitable resistor for an infinitely thin heater source for conducting the THWM as mentioned from the derivation of Nagashima and Nagasaki [32]. Researchers has also investigated that the isonel material does not affect the heat transfer from the wire to the substance due to the electrical insulation [15, 17, 18].

4.1.2 Selection of platinum wire size

As the THWM utilizes a very thin resistor, the AWG size of the platinum wire must be considered. The platinum wire must register a reasonable resistance value as the THWM relies

on the incremental change in temperature of the wire. With a large reasonable resistance of the platinum wire, the change in voltage can be detected for the designed apparatus. To ensure that the cross-sectional area of the platinum wire does affect the predicted resistance, the electrical resistivity equation is used. The electrical resistivity equation helps to determine what the resistance of the platinum wire will be if a specific wire gauge and length was used.

The electrical resistivity ρ_{res} of platinum is $10.6 \times 10^{-8} \Omega m$ [43] to ensure the resistance is obtained for the corresponding resistor. As the cross-sectional area increases, the resistance will decrease as there is more room for electrons to flow. If the cross-sectional area of the wire decreases, then the resistance will increase as the concept to determine a specific wire that is a specific material

4.2. Copper apparatus

A machined copper block was used for the THWM. As copper is known for its high thermal conductivity as a bulk material, integrating a heat source on the outer surface area of the apparatus would allow the fluid/material to maintain a constant temperature during experimental trials that require to extract thermal conductivity at different temperatures. The copper block contains a cavity that will implement for where the substance of interest will be dispensed.

Figure 4.2 illustrates the designed copper piece for the designed cavity.

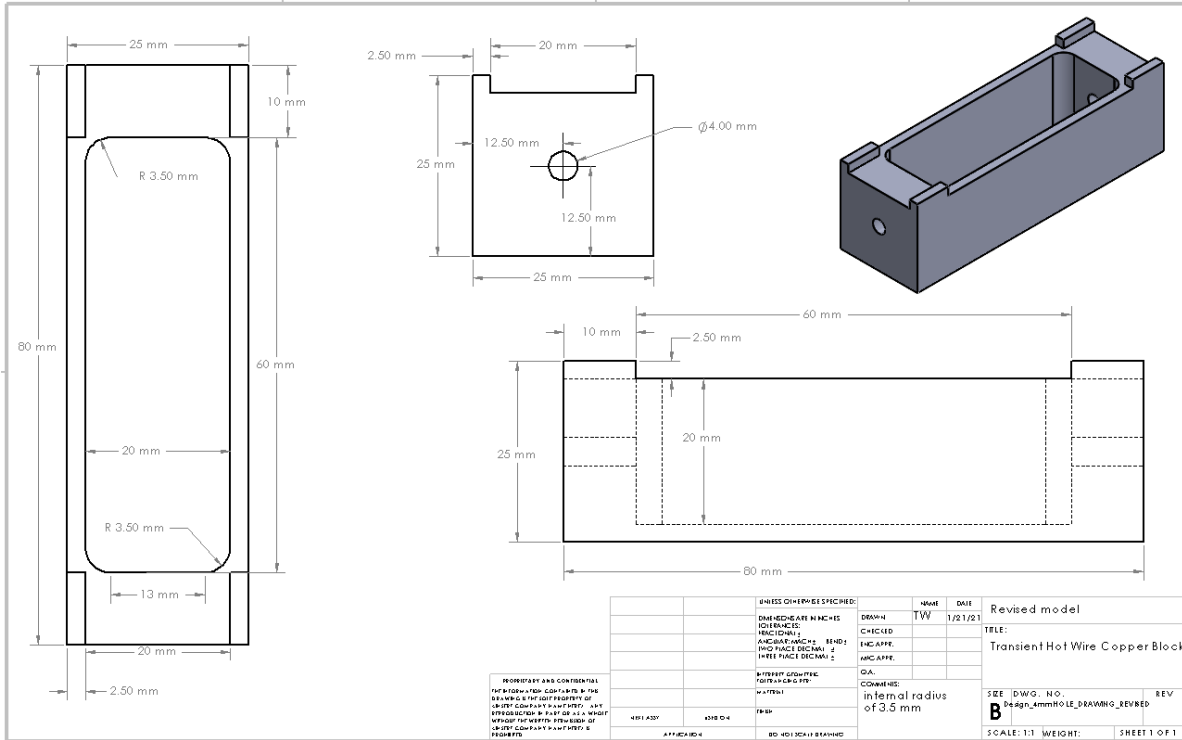


Figure 4.2. SolidWorks drawing of designed copper apparatus

The design of the copper block was based off the literature work [28] with a few touches towards the cavity dimensions to accommodate any challenging techniques to incorporate the platinum wire within the test cell. To ensure that the substance of interest is in contact with the copper cavity during the THW test (to determine TPD), a machined copper piece was integrated with the main vessel. Figure 4.3 provides a general schematic of the copper cover for the THW test cell.

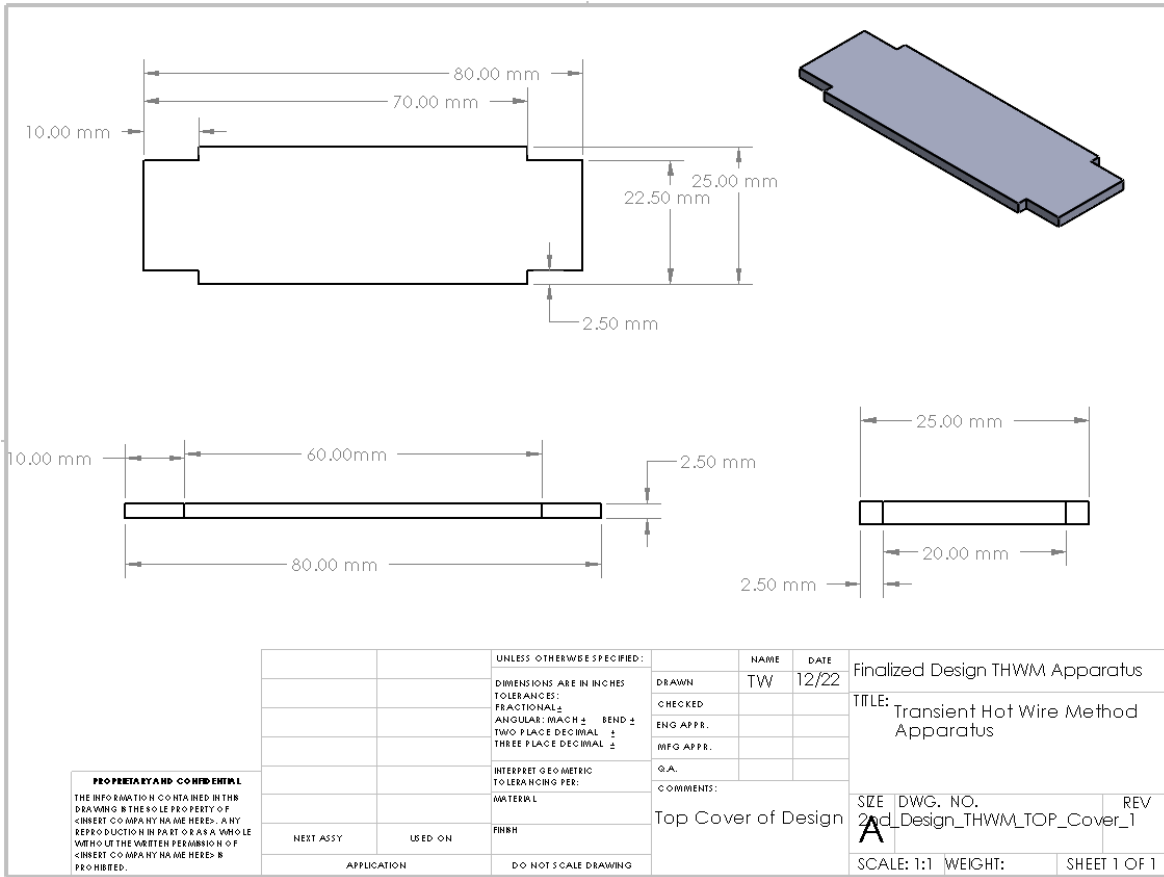


Figure 4.3. SolidWorks drawing of designed copper apparatus cover

4.3. Electronic systems for THW apparatus

The critical systems used for the THWM was a current source, a data acquisition (DAQ) system, and a voltage amplifier. First off, a current source was used to allow the apparatus to produce a constant current over time during the THW test. The model Keithley 6221 current source was used and has the capability to connect with MATLAB utilizing the GPIB to USB port. The restriction for utilizing this specific current source was the operatable ranges of 0-105mA. Even with the current limit, the THWM should work as the overall electronic configuration is similar to two apparatus designs [11, 15].

Next, a DAQ board was used to detect the voltage drop of the platinum wire. The USB-1808 DAQ board has the capability to detect 0.07mV with an analog to digital resolution of 18 bits. was used to register the voltage drop in either differential or single ended modes. The differential mode was used to ensure that the signal from the positive and negative lead cancels out any electrical noise from the signal during the experiment to produce a transient curve as a Heaviside step current was used to perform the THW test. The DAQ board is in line with the MATLAB code as the current source allows the specific electrical current to initiate the test and the DAQ board to register the voltage readings (shown in Appendix B.1). However, with only the DAQ board able to extract raw voltages and provides no low pass filters, a clear signal must exist to extract the transient voltage drop of the platinum wire.

Lastly, a Stanford Research 560 System low noise voltage preamplifier was used adjacent to the DAQ board. This ensures that a large amount of current would not have to be used to detect the voltage drop of the platinum wire and overcomes any electrical noise within the data extraction. With the right optimal voltage gain without any overloading, the data can be traceable to illustrate the temperature rise of the platinum wire in the THW test cell. Overloading the THW test cell will provide no accurate results as the voltage amplifier is able to register 5-6 volts maximum with the amplification. Anything passing 6V results to an inaccurate measurement where the data does not increase exponentially from the applied Heaviside step current for the THW test.

4.4. Copper leads

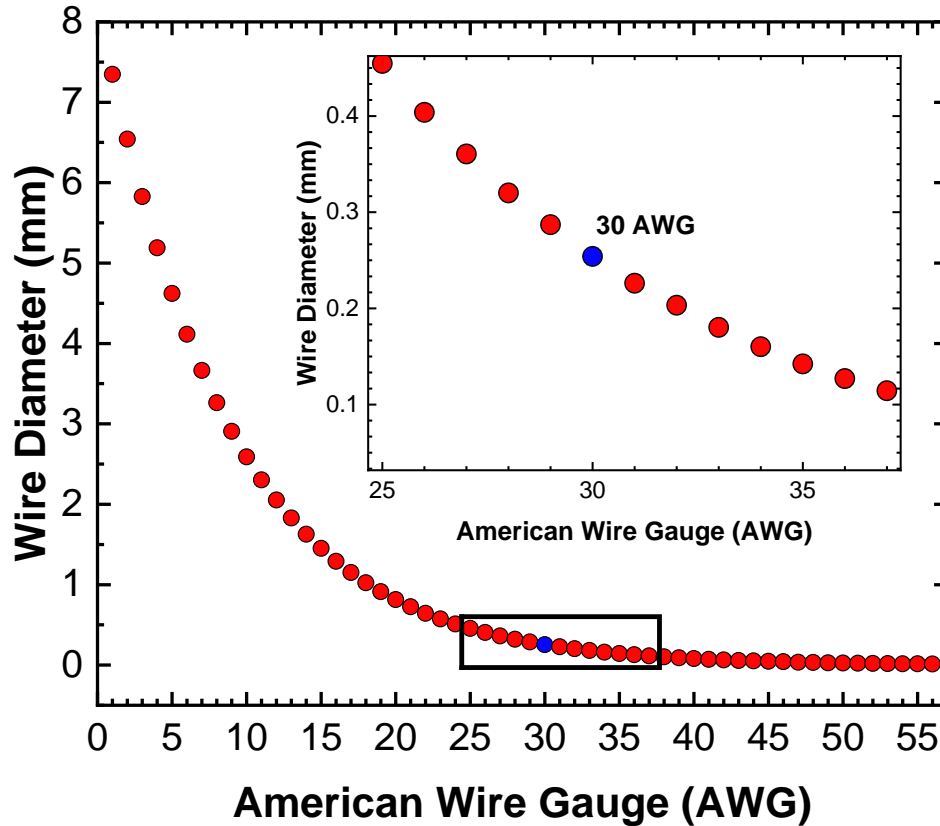


Figure 4.4. Plotted wire diameters corresponding to AWG with a close-up view of 30 AWG.

Data from [42]

Insulated 30 AWG copper leads were used to help connect the platinum wire to the current source and voltage amplifier. From figure 4.4, 30 AWG has a larger diameter comparing to the 50 AWG platinum wire (from section 4.1.1). A 30 AWG wire is approximately 0.25mm in diameter which is 10 times larger than a 50 AWG wire (referring to selected platinum wire diameter). 30 AWG wires were used due to the restricted dimensions of what the DAQ system was capable to detect (from 18-30 AWG wires). As the entire setup is configured in a 4-wire connection, two copper leads would be attached to each end of the platinum wire to fulfill the

electrical circuit to measure fluid's thermal conductivity. The 4-wire configuration allows the resistor of interest to obtain its accurate resistance due to the noncontributing resistance from the copper leads. The copper lead sizing was another factor to accommodate for the inner diameter of the PTFE tube which was 2mm. However, two 30 AWG copper leads were able to slide within the PTFE tube easily (from modeling the wires out in SolidWorks prior to ordering the materials).

4.5. Configuring platinum wire

As the main purpose of the THWM is to utilize a thin platinum wire, soldering was vital. With a wire diameter at 25 μm , conventional techniques to solder a wire cannot be used. With a thin coating of isonel insulation, burning off the material helped to expose the bare wire. This helps to ensure that the copper leads are connected to the platinum wire. Figure 4.5 shows the process of removing the insulation from the thin platinum wire.

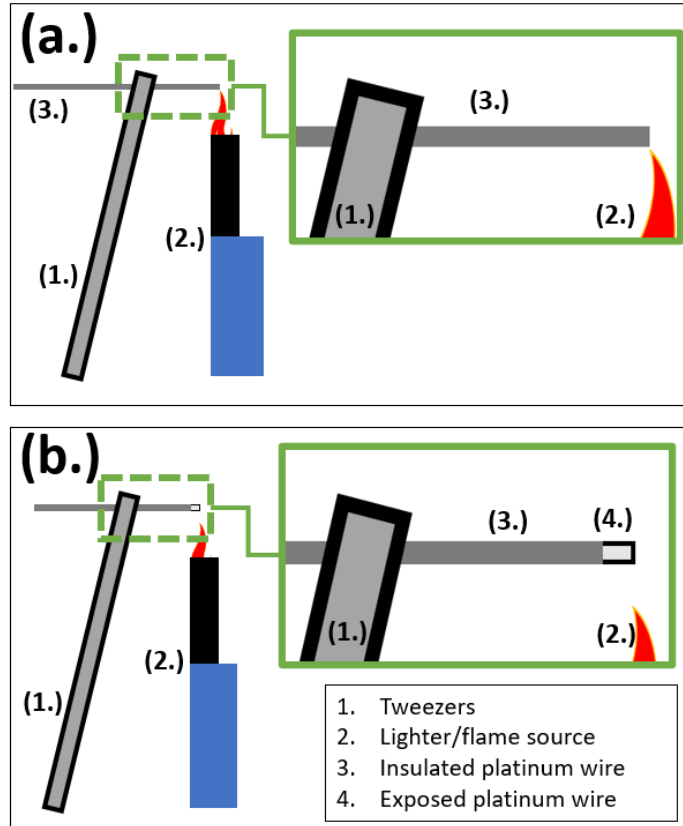


Figure 4.5. Illustration to remove platinum wire's insulation

After removing the platinum wire's insulation, soldering was approached differently. The copper wires from each end of the copper vessel were coated with solder first. With the high potential of the 25 μm diameter wire snapping off easily, tweezers were used to hold the platinum wire close to the soldered node of the copper leads. With the soldering iron in contact with the tinned copper leads, the heat allows the solder to transition from solid to liquid. This provides the platinum wire to contact the copper leads within the liquid metal and solidifies to ensure a steady electrical connection was made. This was done on the opposing side of the platinum wire to span within the copper cavity. Figure 4.6 shows the overall technique to solder the platinum wire.

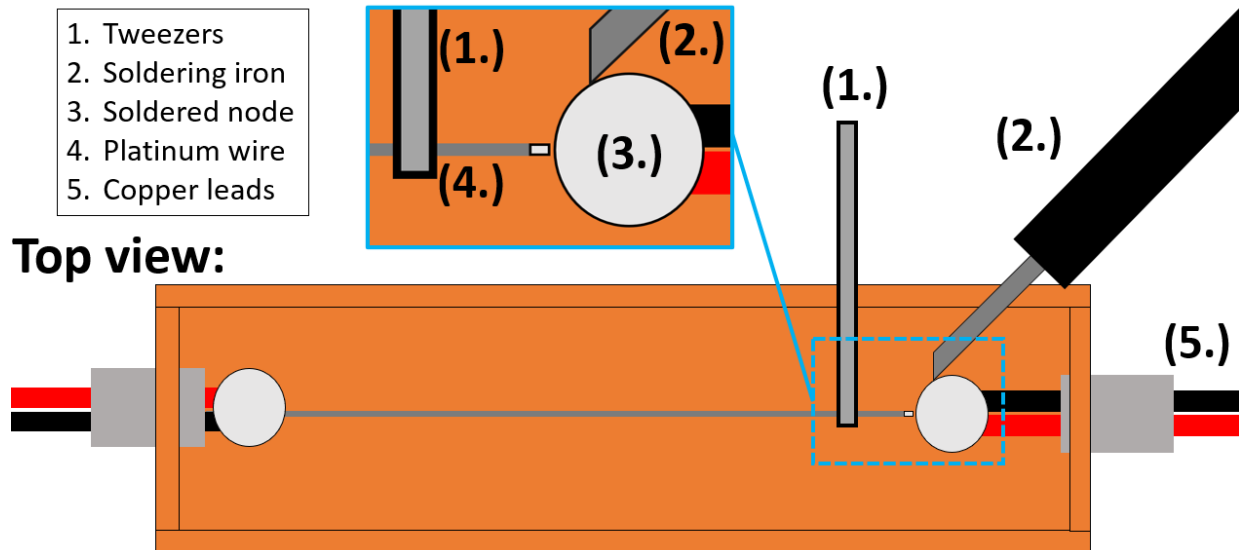


Figure 4.6. Top view of soldering technique within copper cavity

After soldering, a solid connection must exist between the copper leads and the platinum wire. Utilizing a digital multimeter (DMM) provided an insight of how the platinum wire showed a consistent/inconsistent reading in its resistance with the two-probe technique. Figure 4.7 shows the overall approach of how the designed THW test cell was measured with the DMM to ensure a solid resistance reading after soldering. If an inconsistent resistance reading is shown from the DMM, then the soldering technique was repeated until a steady resistance reading is displayed. To ensure that the displayed resistance of the platinum wire was correct, the resistivity equation (equation 4.1) was utilized to determine if the resistance is close to the theoretical resistance value of the soldered platinum wire.

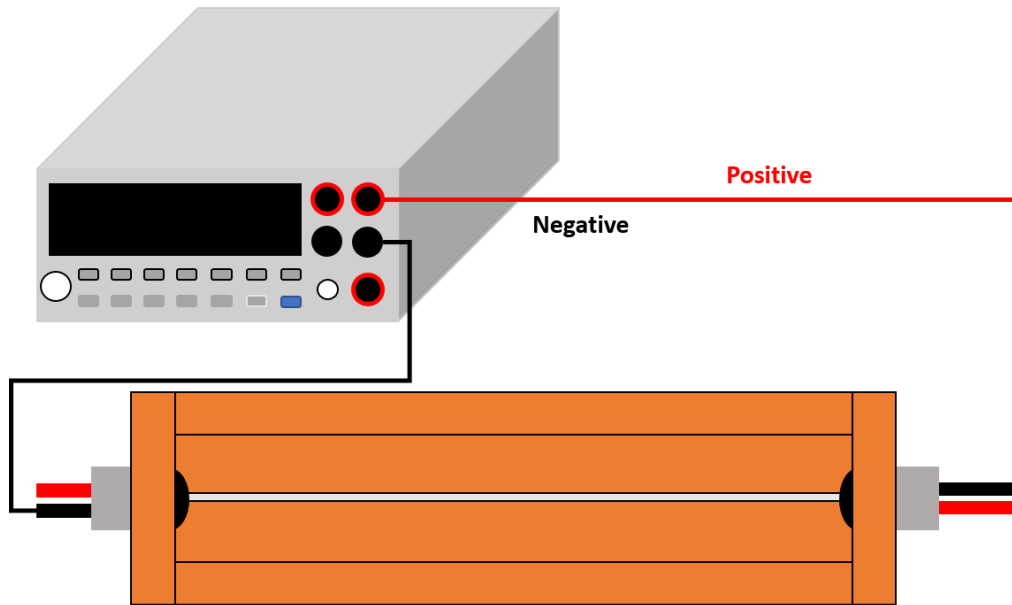


Figure 4.7. Two-probe technique after soldering platinum wire

4.5.1 Insulation test

With a solid connection of the platinum wire and copper leads, epoxy was added around the surface area of the entire electrical nodes of the platinum wire and copper leads. With one day of a full cure time for the epoxy to harden, liquid electric tape was also applied to the cured nodes. This ensures the electrical nodes to be perfectly insulated as it operates exactly like electric tape but in a liquid form to cover tiny areas to electrically insulate the applied solid surface from conductive materials/substances. Approximately five coating of liquid tape were used for the nodes. To also illustrate that the electrical nodes were insulated from any current leakage, a two-probe technique was used to illustrate that no current was flowing within the liquid medium (DI water). Figure 4.8 shows the simple schematic behind the two-probe method where the positive lead connects to the copper wire (from any leads outside of the copper apparatus) and the negative lead was dipped into the liquid to display a resistance reading. The

two-probe technique was also done vice versa to ensure that current should not flow between the electrical nodes due to the layering of epoxy and liquid electric tape as an insulation barrier.

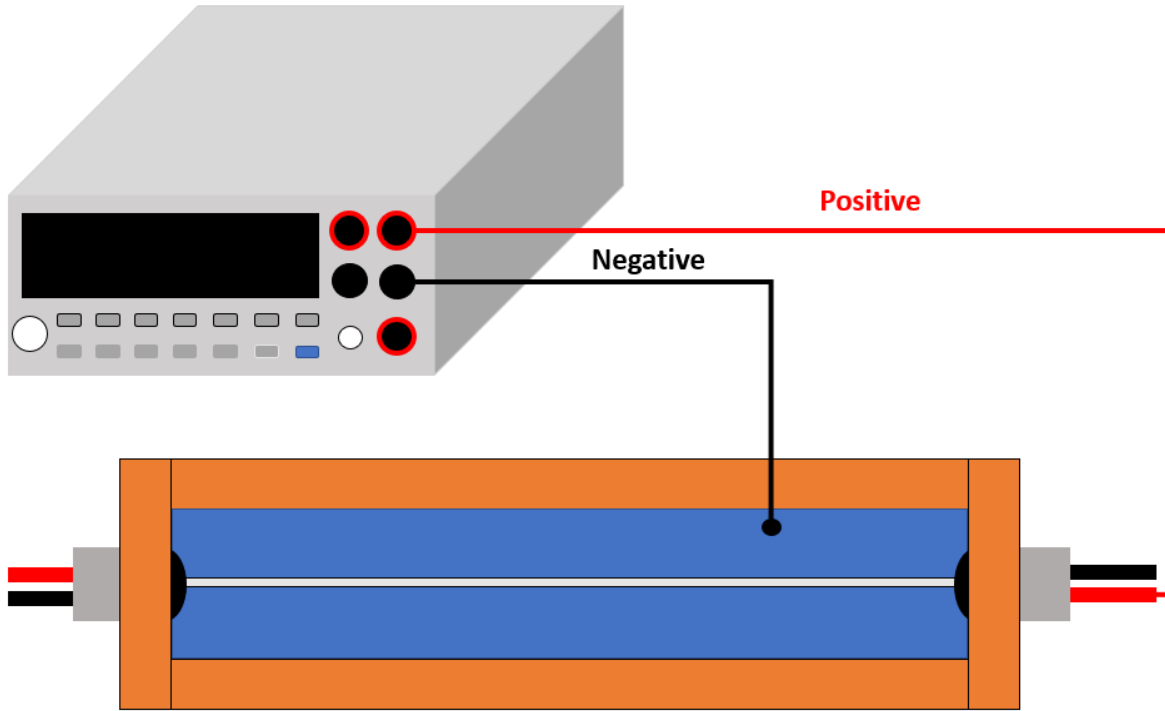


Figure 4.8. Two-probe technique where the positive lead connected to copper wire and negative lead dipped in liquid

4.6. Apparatus setup

With all the necessary equipment and materials integrated together, the apparatus has been developed. The current source and DAQ board work in synchronous with each other through the MATLAB code (shown in appendix C). The voltage amplifier was manually set to 100hz as the cutoff filter, the low pass filter with 12dB/Octave roll off was utilized to ensure the lower frequencies are capable to pass through the amplifier. The gain mode was selected to low noise and the appropriate voltage gain was manually selected to prevent any voltage overload. The voltage amplifier system itself provided gain selections ranging from 1, 2, and 5 by factors of 10^1 , 10^2 , 10^3 , and 10^4 . The highest and lowest gains used in this thesis were 200 and 5,

respectively without any type of overloading. The voltage gains of 200, 20, 10, and 5 were used for the TCR measurement, detecting the change in voltage of air, detecting ethanol's and IPA's change in voltage, and detecting water's thermal conductivity, respectively. The overall platinum wire's length is 38.5mm within the 60mm long copper cavity to allow the wire to be completely submerged for the THW test. The necessary connections from the DAQ board and current source are connected to the laptop with the necessary USB connections. Figure 4.9 shows the entire setup of the designed THW test bench.

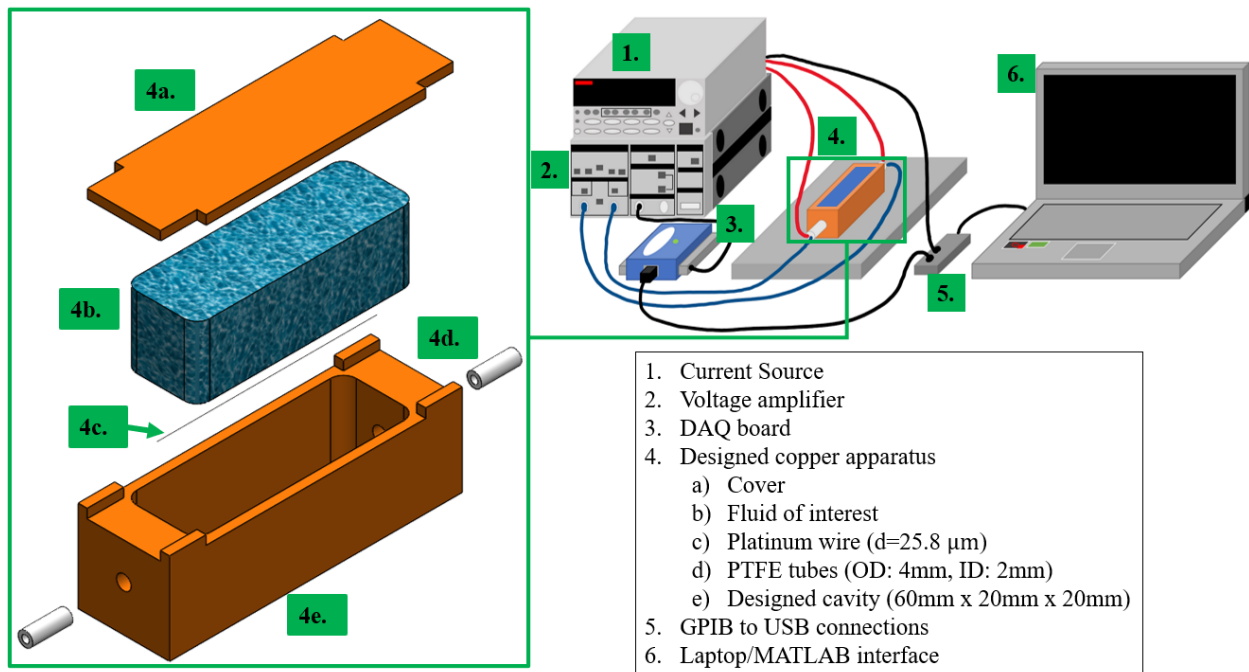


Figure 4.9. Developed transient hot-wire setup

Chapter 5. Temperature coefficient of resistance of platinum wire

This chapter will discuss critical testing approaches to ensure the developed THW test cell is able to operate correctly before measuring any fluid's thermal conductivity values.

5.1. Overall setup of TCR measurement

Once the apparatus is confirmed to be electrically insulated, extracting the TCR of the platinum wire is the next step. The THW apparatus is dependent on the resistance of the platinum wire which also exhibits its change in temperature over time as mentioned from chapter 3. The literature TCR value of pure platinum is 0.003927 K^{-1} at ambient temperature [44]. The resistance of the insulated platinum wire will change when the temperature of the wire is either higher or lower than ambient temperature. The platinum wire configured in this thesis is 38.5 mm in length spanned within the copper cavity. With the use of DI water as the main liquid, the wire shows that the temperature of the fluid is exactly the temperature of the thin wire. Configuring the setup with the 4-wire technique, a small current value was utilized throughout the TCR experiment. A gain of 200 was utilized during the TCR experiment for the voltage amplifier. When the liquid was at a higher temperature, there were no signs of any voltage overloads which helps to extract the amplified data of the platinum wire. The amplified voltage was then divided by the corresponding voltage gain to extract the correct voltage from the platinum wire where the low current passes through the thin resistor. With constant current in the loop, the experimental approach was to measure the voltage drop of the wire adjacent with the corresponding temperature of the liquid with the thermocouple data logger. Figure 5.1 illustrates the overall setup to conduct the TCR experiment.

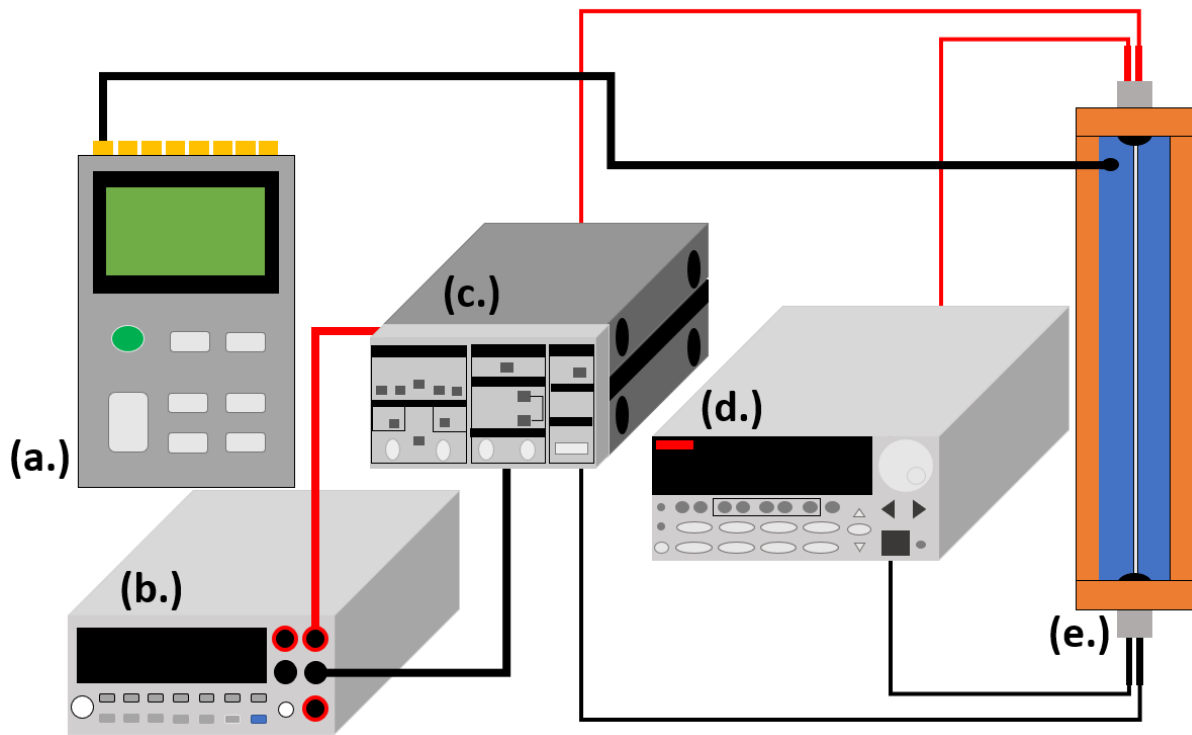


Figure 5.1. TCR setup: (a.) thermocouple data logger, (b.) DMM, (c.) voltage amplifier, (d.) current source, (e.) copper apparatus with water

5.2. Obtained TCR of 50AWG platinum wire

With the data obtained, the temperature and resistance of the platinum wire were plotted in an XY plot to investigate the linearity. This will provide a linear regression of the overall platinum wire and will produce a slope corresponding to the change in resistance over the change in temperature. Figure 5.2 illustrates the obtained resistance values of each corresponding temperatures.

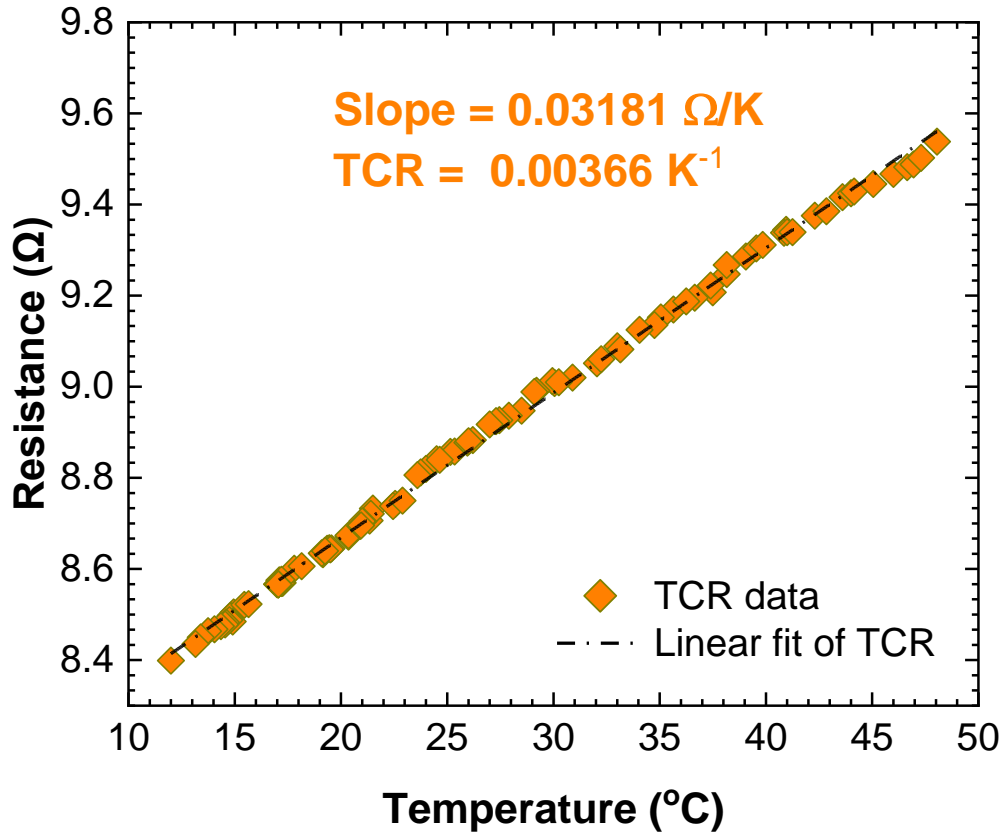


Figure 5.2. Platinum wire's temperature coefficient of resistance

To obtain the TCR value of the platinum wire at ambient temperature (22°C), equation 5.1 was used which is:

$$\alpha_{TCR} = \frac{Slope_{TCR}}{R_{ref}} \quad (5.1)$$

The variables α_{TCR} , $Slope_{TCR}$, and R_{ref} are the TCR value at the corresponding temperature, the slope of the change in resistance over change in temperature (0.03181 Ω/K), and the referenced resistance at the referenced temperature ($R_{ref}= 8.77\Omega$ at 22°C), respectively. The TCR value at 22°C resulted in 0.00366 K⁻¹. To compare with other literature studies towards the platinum wire calibration test, pure platinum's TCR is 0.003927 K⁻¹ [44] which indicates a

difference of 7.3% from the extracted value of 0.00366 K^{-1} . Another referenced TCR value from a calibrated THW test bench from Wei et al. is 0.003792 K^{-1} [28] which also shows that the percent difference is equivalent to 1.9%. As Wei's 50 AWG platinum wire is coated with the same isonel material, this shows that the TCR value is in reasonable range to utilize towards the customized designed THW test bench.

Chapter 6. Transient hot-wire method results

6.1. Experimental approach for THW apparatus

From extracting the necessary TCR of the 25 μm diameter platinum wire, the experiment can be conducted with all the equipment connected and work in synchronous. First the current source was selected to trigger a constant input through the designed THW circuit. Current ranges from 20-95mA were used to help detect the voltage drop of the platinum wire. It was found that materials with a higher k value, requires higher current to detect the change in voltage during the THW test [28]. Even as the THW apparatus is detecting exceedingly small voltages, the low noise amplifier was used to overcome the electrical noise from applying the Heaviside step current. With the right gain and the low noise filter, the voltage detection was much clearer to view over the entire test period. With the DAQ board capable of detecting 50kHz as the maximum sampling rate, 1kHz was used in the THWM. This was to investigate how the temperature response of the platinum wire will be over a 10 second interval for different fluids. This will also illustrate where the initial wire heating takes place and the onset of convection during the THW test. With lower sample rates, it was experimentally investigated that determining the initial wire heating phase does not appear as it typically occurs at shorter durations. To ensure that the initial wire heating is viewed and avoided for fitting in the line of best fit, it was necessary to conduct the experiment with 1kHz. In between the wire heating phase and convection region, a linear regression will appear to indicate that the joule heating effect is constant for a short period of time. This region specifically is where the least square method is used to extract the thermal conductivity of the medium [39].

Since the designed THW apparatus experimental duration is done in 10 seconds, conducting 10 trials with the same parameters for each fluid was done. This was to help reduce the

signal noise of the obtained experimental trials for different fluids. The fundamental equations to utilize for obtaining the average, standard deviation and, standard error of mean (SEM) [45]. First off, the average equation:

$$\bar{x} = \frac{\sum_{i=1,2,\dots,n}^n x_i}{n} \quad (6.1)$$

The variables \bar{x} , $\sum_{i=1,2,\dots,n}^n x_i$, and n represents the average value of all conducted trials, the sum of all data values, and the number of data items in the sample, respectively. With obtaining the average the standard deviation can be calculated with:

$$\sigma = \sqrt{\frac{\sum_{i=1,2,\dots,n}^n (\bar{x} - x_i)^2}{n-1}} \quad (6.2)$$

The variables σ , $\sum_{i=1,2,\dots,n}^n (\bar{x} - x_i)^2$, and n represents the standard deviation of the data set, the sum of all data values squaring the difference between the average of the overall data set and conducted sample trial, and the number of data items in the sample, respectively. With the use of equation 6.2 to extract the standard deviation, SEM must be calculated which equates to:

$$\sigma_{SEM} = \frac{\sigma}{\sqrt{n}} \quad (6.3)$$

The variables σ_{SEM} , σ , and n represents the overall SEM of the analyzed average samples of data, the overall standard deviation, and the number of data items in the sample, respectively.

Utilizing equations 6.1-6.3, Excel was used to obtain the average, standard deviation, and SEM of the analyzed thermal conductivity values from the conducted THW test.

The raw data trials obtained were the corresponding voltage drop of the platinum wire of the duration of 10 seconds. The voltage values were converted to resistance and then to

temperature implementing Ohms Law and the TCR equation, respectively (shown from chapter 3).

6.2. Preparing THW apparatus before testing

To operate the THW apparatus the fluid must be dispensed within the vessel. The day prior to operating the test cell, the cavity is cleaned up with soapy water, isopropyl alcohol, and rinsed with DI water. This is to remove any residue of the test sample from operating a full day of the THW apparatus and allowing the platinum wire to be sequentially clean. After draining out the liquid from the cell, the vessel was air dried over night to allow the moisture within the apparatus to evaporate. When testing with only air or water, the cleaning procedure is not necessary. If different fluids such as oils, powders, or glycol-based solutions were used, then the cleaning procedure is necessary for the platinum wire and cavity walls to remain clean.

6.3. THWM for air

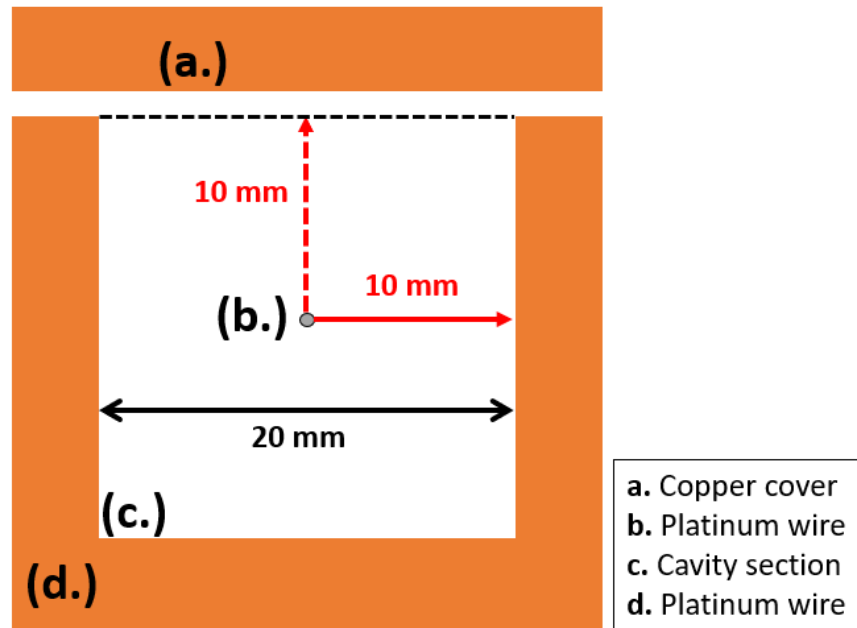


Figure 6.1. Front cross-sectional view of the designed copper cavity to reference radial distance for TPD.

The first fluid of interest to test was air. It has been known that air is the perfect insulator due to its low thermal conductivity approximately 0.026 W/mK (shown in appendix A table A.2) at ambient temperature [6, 41]. To ensure accurate readings of the platinum wire during the THW test, a cover was placed above the copper apparatus to ensure that the heat diffused from the wire in the radial direction does propagate uniformly towards the solid walls of the cavity as shown in figure 6.1. To ensure that the wire can detect air's thermal conductivity, TPD was calculated. For air, the TPD is about 9.4mm at 1 second. This means that the heat diffused in the radial direction from the wire is almost equivalent to the radial distance of the copper cavity. The time range to fit in the data to extract air's thermal conductivity was less than 1 second to ensure there was no signal disturbance from the wire to the copper walls of the apparatus. However, to ensure that the TPD signal interference existed for air, each trial was conducted in 10 seconds.

Air was measured with an input of 20mA with the appropriate voltage gain of 20. With the utilization of the TPD, 20mA was the right current input to allow enough heat to raise the temperature of the wire roughly by 1 K over the 10 second interval. It was also shown that the initial wire heating did occur from the onset of the trials and the signal interference after the time duration of the TPD occurred. The THW test was done 10 times with the same configuration to detect air's thermal conductivity. Data analysis to extract the averaged data set of the substance and plotting the thermal conductivity extraction graph can be viewed in Appendix B.2 and B.3, respectively. Figure 6.2 is the averaged extraction of the 10 conducted data sets to detect air's thermal conductivity. The plot is similar to Wei et al. thermal conductivity extraction process [28] in which $\frac{4\pi\Delta T}{q'}$ and $\ln(t)$ were plotted as the Y and X axis, respectively. Obtaining the overall slope from the $\frac{4\pi\Delta T}{q'}$ vs $\ln(t)$ plot would allow the result to be in the units of $W^{-1}mK$ which is the inverse of the thermal conductivity units. Taking the inverse of the extracted slope will provide the extracted value of the substance's thermal conductivity in the THW test cell. The time intervals of 0.3 to 0.8 seconds were fitted along the linear regression as the earlier time duration illustrates the initial wire heating phase and the convection region occurred close to 0.9-1 second mark from the 10 second experiment. TPD was also accommodated as it was in the region where convection occurred after the 1 second mark.

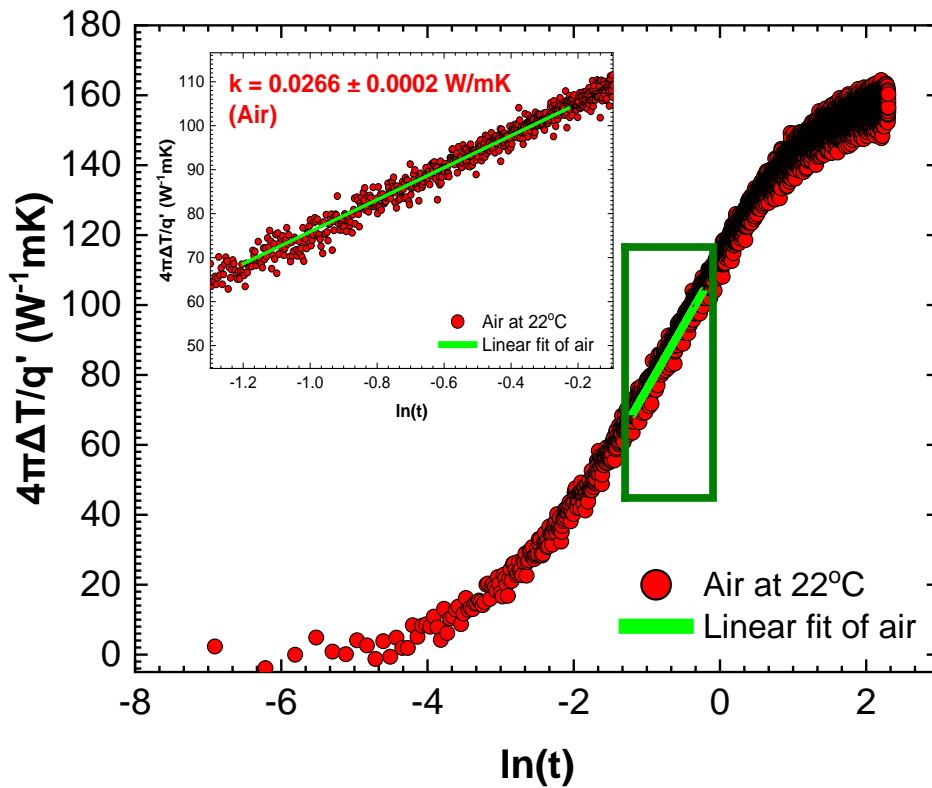


Figure 6.2. Data obtained from THW apparatus for measuring air

From the 10 conducted trials in table 6.1, it is shown that air's thermal conductivity does fluctuate from 0.0255 W/mK to 0.0274 W/mK as the lowest to highest extracted values, respectively. From averaging the 10 trials of the raw voltage data to convert to temperature the extracted value of air's thermal conductivity is $0.0266 \pm 0.0002 \text{ W/mK}$. From comparing the literature value of air at 0.0259 W/mK at 22°C [6, 41], the experimentation does indicate a 2.6% difference concluding a reasonable range to detect the thermal conductivity of air. From analyzing air's thermal conductivity, the time range of 0.3 to 0.8 seconds were selected to accommodate the initial wire heating phase, convection range, and TPD. With those specific time ranges, the change in temperature is approximately 0.27°C (or 0.27 K) which indicates that

the wire's temperature rise is relatively low but corresponds to the joule heating effect needed for the platinum wire to transfer heat constantly to the measured substance.

Table 6.1. Experimental trials from THWM measuring air at 22°C vs referenced value

| Trials | Extracted thermal conductivity (W/mK) | Percent error (%) at 0.0259 W/mK [6] |
|---|--|---|
| 1 | 0.0268 | 3.358 |
| 2 | 0.0255 | 1.569 |
| 3 | 0.0274 | 5.474 |
| 4 | 0.0261 | 0.766 |
| 5 | 0.0274 | 5.474 |
| 6 | 0.0265 | 2.264 |
| 7 | 0.0262 | 1.145 |
| 8 | 0.0271 | 4.428 |
| 9 | 0.0265 | 2.264 |
| 10 | 0.0264 | 1.894 |
| Avg | 0.0266 | 2.632 |
| Standard deviation σ | 0.0006 | - |
| σ_{SEM} | 0.0002 | - |

6.4. THWM for isopropyl alcohol

The second fluid of interest was isopropyl alcohol (IPA). IPA's thermal conductivity from literature is approximately 0.1357 W/mK at ambient temperature [47] which is higher than air's thermal conductivity. From the first test with air, we utilized the temperature rise between the time range of 0.3 to 0.8 seconds to be 0.27°C. To ensure we aim for a temperature rise of 0.27°C within the time range of 0.3 to 0.8 seconds, an input current of 45mA was utilized. This was to ensure that the platinum wire is capable to provide a constant change in temperature closely to how air was obtained but utilizing a higher current input to detect the necessary voltages over time from the Heaviside step current. It was also hypothesized from reverse calculating what input current shall be used within the derived heat equation for the THW test cell to obtain the referenced thermal conductivity value of IPA. Ten trials of measuring IPA at 22°C with the same configuration are shown in table 6.2. cell to obtain the referenced thermal conductivity value of IPA. Ten trials of measuring IPA at 22°C with the same configuration are shown in table 6.2. The lowest and highest extracted values for IPA's thermal conductivity was 0.1282 W/mK to 0.1576 W/mK, respectively. From applying the same method to plot out the thermal conductivity extraction graph, the reported value of IPA from the THW test is 0.1425 ± 0.0031 W/mK (shown in figure 6.3). Comparing to literature value of 0.1357 W/mK [6], the two values differ by 5.2%.

Table 6.2. Experimental trials from THWM measuring IPA at 22°C vs referenced value

| Trials | Extracted thermal conductivity (W/mK) | Percent error (%) referenced at 0.1357 W/mK [47] |
|---|--|---|
| 1 | 0.1387 | 2.163 |
| 2 | 0.1399 | 3.002 |
| 3 | 0.1540 | 11.883 |
| 4 | 0.1306 | 3.905 |
| 5 | 0.1282 | 5.850 |
| 6 | 0.1489 | 8.865 |
| 7 | 0.1395 | 2.724 |
| 8 | 0.1413 | 3.963 |
| 9 | 0.1576 | 13.896 |
| 10 | 0.1526 | 11.075 |
| Avg | 0.1425 | 4.772 |
| Standard deviation σ | 0.0099 | - |
| σ_{SEM} | 0.0031 | - |

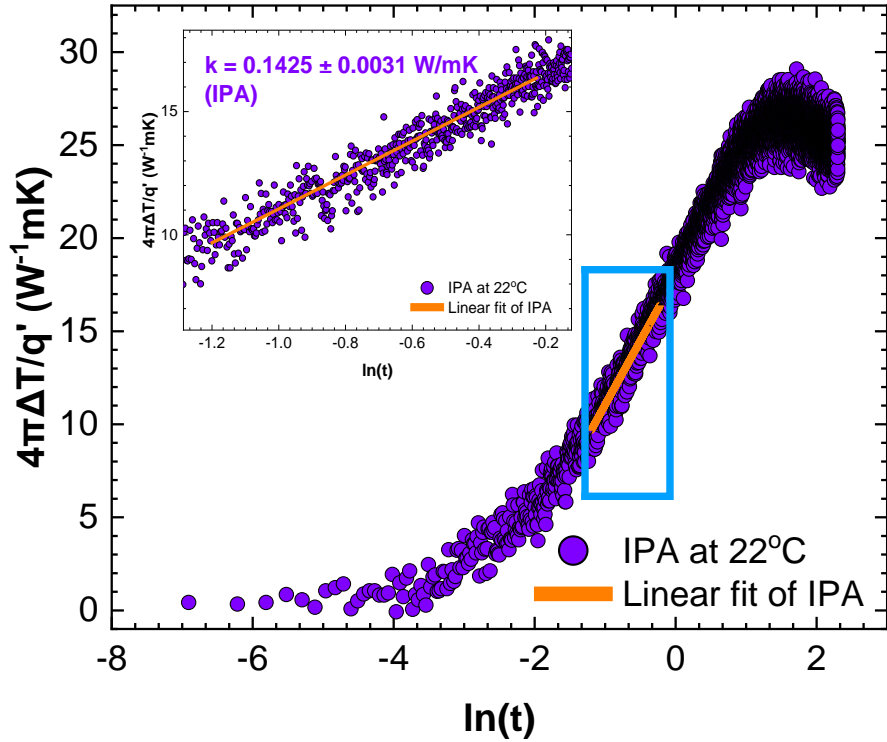


Figure 6.3. Data obtained from THW apparatus for measuring IPA

6.5. THWM for ethanol

The third fluid of interest was ethanol. Ethanol's thermal conductivity value from literature is 0.1698 W/mK [48]. As IPA was tested as the liquid with the lowest thermophysical property, ethanol does have a slightly higher thermal conductivity value and was a good candidate to investigate if the THW test worked or not. To investigate that the thermal conductivity of ethanol would require a different electrical current input, the suggested current was 50mA to compensate the temperature rise of 0.27°C within the time range 0.3 to 0.8

seconds. Table 6.3 shows the extracted data of obtaining ethanol's thermal conductivity and illustrates that using the predicted current led to some fluctuated extractions of the thermophysical property. Ranges of 0.1629 W/mK to 0.1967 W/mK were the lowest and highest extracted values for ethanol from observing table 6.3.

Table 6.3. Experimental trials from THWM measuring ethanol at 22°C vs referenced value

| Trials | Extracted thermal conductivity (W/mK) | Percent error (%) referenced at 0.1698 W/mK [48] |
|---|--|---|
| 1 | 0.1815 | 6.446 |
| 2 | 0.1679 | 1.132 |
| 3 | 0.1763 | 3.687 |
| 4 | 0.1967 | 13.676 |
| 5 | 0.1802 | 5.771 |
| 6 | 0.1629 | 4.236 |
| 7 | 0.1782 | 4.714 |
| 8 | 0.1712 | 0.818 |
| 9 | 0.1805 | 5.928 |
| 10 | 0.1770 | 4.068 |
| Avg | 0.1768 | 3.959 |
| Standard deviation σ | 0.0091 | - |
| σ_{SEM} | 0.0029 | - |

With the same approach to plotting out the extracted thermal conductivity graph of air and IPA, ethanol's data can be viewed from figure 6.4. From the 10 analyzed experimental trials for ethanol, the averaged extracted thermal conductivity value of came to be 0.1768 ± 0.0029 W/mK. Comparing to literature [48], the experimental and expected value differ by 4.2%.

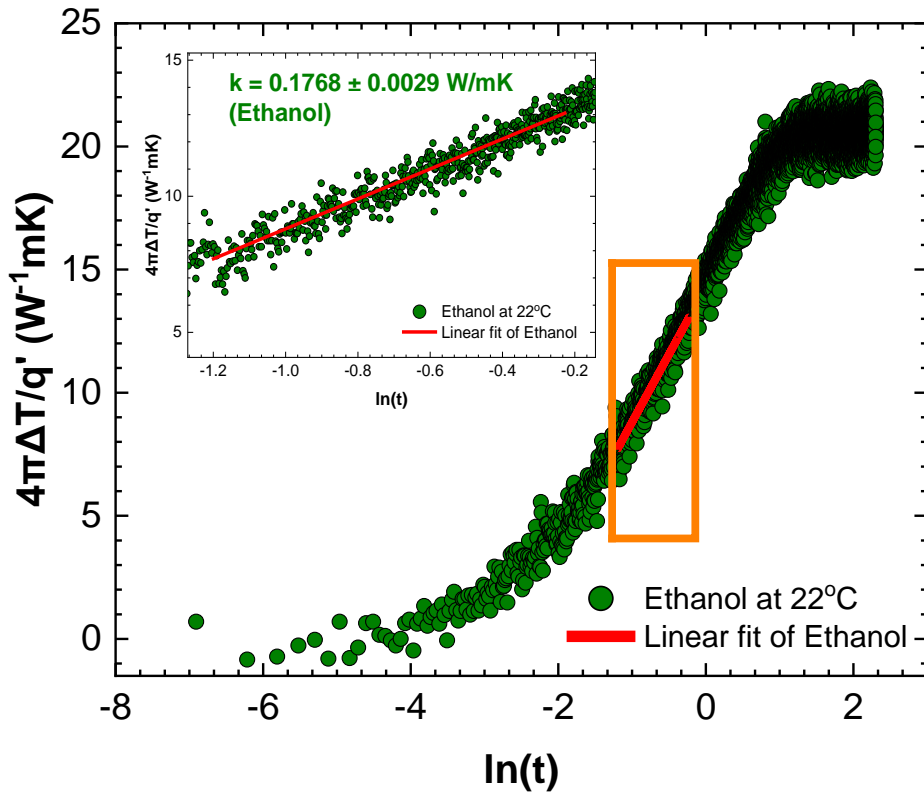


Figure 6.4 Data obtained from THW apparatus for measuring ethanol

6.6. THWM for deionized (DI) water

The fourth fluid of interest was DI water. Utilizing DI water indicates that the substance is pure water, and no impurities are present in the liquid medium. As water has the highest thermal conductivity out of the three measured substances, its literature value is between 0.59-0.60 W/mK [6, 36] at ambient temperature (also shown in appendix A). With the same principle to determine the input current with IPA and ethanol, water's expected input current was 95mA. Conducting 10 trials for 10 seconds, the data extracted were consistent and the averaged reported thermal conductivity of water was 0.6007 ± 0.0048 W/mK as shown in figure 6.5.

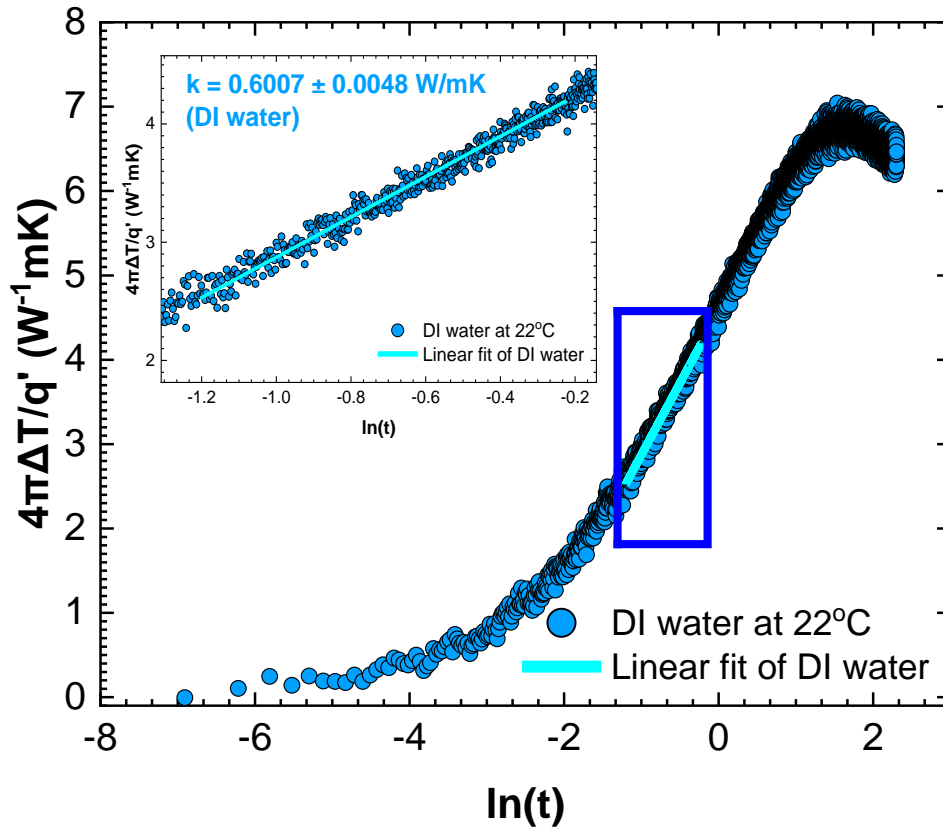


Figure 6.5. Data obtained from THW apparatus for measuring DI water

Table 6.5 shows that the results of the experimental values and literature values are in tolerable ranges as the literature value of water is in good agreement. The largest and lowest reported value for water were 0.6173 W/mK and 0.5833 W/mK, respectively. From comparing the overall reported thermal conductivity value of DI water, the experimental and literature [6, 44] differ less than 1%. This indicates that thermal conductivity of DI water is detectable as the wire's temperature rise is within 0.27°C from the fitted time range of 0.3 to 0.8 seconds. Comparing to air's thermal conductivity extraction with the same temperature rise over time with a current input does validate that higher k values require more input current [28].

Table 6.4. Experimental trials from THWM measuring DI water at 22°C vs referenced value

| Trials | Extracted thermal conductivity (W/mK) | Percent error (%) referenced at 0.6014 W/mK [6] |
|---|--|--|
| 1 | 0.5749 | 4.609 |
| 2 | 0.5833 | 3.103 |
| 3 | 0.6154 | 2.275 |
| 4 | 0.5846 | 2.874 |
| 5 | 0.6013 | 0.017 |
| 6 | 0.6173 | 2.576 |
| 7 | 0.6170 | 2.528 |
| 8 | 0.6082 | 1.118 |
| 9 | 0.5997 | 0.283 |
| 10 | 0.6084 | 1.151 |
| Avg | 0.6007 | 0.117 |
| Standard deviation σ | 0.0153 | - |
| σ_{SEM} | 0.0048 | - |

6.7. Validation of the analyzed data

With all four different fluids measured, compiling all the data together would see how each data trend differ from each other. This approach is similar to Wei’s approach to extract thermal conductivity [28]. From conducting each THW test with all four different fluids, the temperature rise, and time range were consistent. On the other hand, as each fluid requires different heat inputs since higher k values require more electrical current [28], the data

regression will show which fluid has a higher or lower slope. From observing figure 6.6, the data region that has the highest slope of $\frac{4\pi\Delta T}{q'}$ vs $\ln(t)$, would result that an insulator has been measured within the THW test cell which illustrates that air was measured. Thermal conductive substances like water would result in a smaller slope resulting in a higher value in thermal conductivity. Substances such as IPA and ethanol would be in close range when comparing their literature and measured experimental thermal conductivity values at ambient temperature.

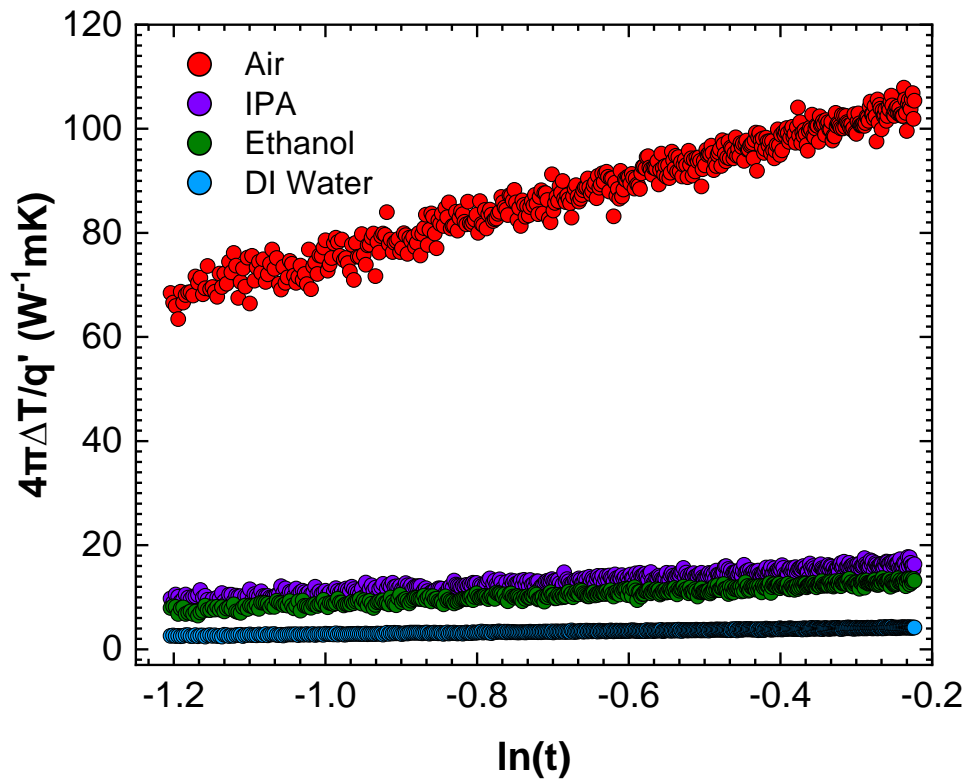


Figure 6.6. compiled data with air, IPA, ethanol, and DI water

Figure 6.7 shows a clear view of the IPA, ethanol, and DI water data. This is to locate which region IPA, ethanol, and DI water would be on the graph as air is clearly shown to have a higher slope regression (leading to a low thermal conductivity value). It is shown that IPA is the

second substance for its low thermal conductivity and the data trend would be above ethanol and water to show that it is an insulative liquid. Lastly, ethanol will show that its thermal conductivity is the third lowest compared to all the remaining fluids tested in this thesis. The data trend for ethanol would be between IPA and DI water.

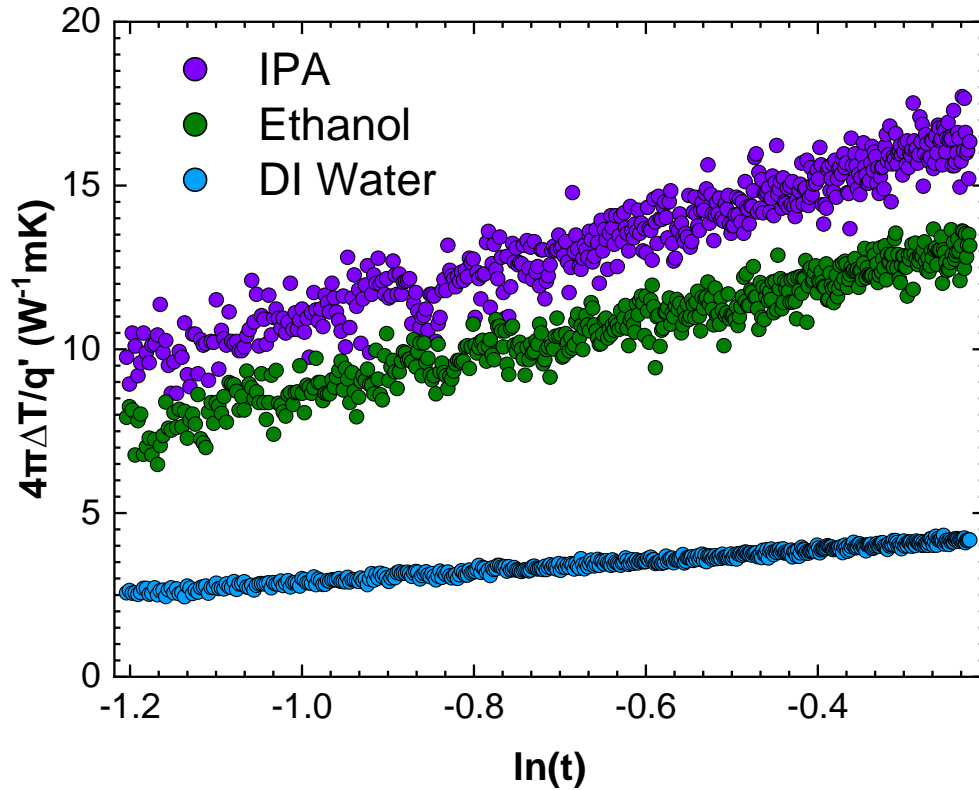


Figure 6.7. Close up view of the compiled data of IPA, ethanol, and DI water.

6.8. Discussion

With all 4 tested substances measured in the THW test cell, it is shown that the designed apparatus is highly capable to detect thermal conductivity of fluids. The temperature rises from conducting air and water separately were in the range of 0.27°C to fit within the time range of 0.3 to 0.8 seconds with a percent error of 2.632% and 0.117%, respectively. With traces of IPA

and ethanol evaporating over time in the covered test cell, this could be the potential to the larger percent error of 4.772% and 3.959%, respectively. Evaporation was mentioned because when the THW test cell was complete for their corresponding fluid, the liquid level did decrease slightly once the copper cover was lifted to draw the liquid back into its corresponding vial. Water did not have the tendency to evaporate quickly compared to IPA and ethanol. which may have contributed to a low percent error from the THW test. Overall, the obtained data from the designed THW apparatus can detect fluid's thermal conductivity with utilizing the current input to extract the desired temperature range of 0.27°C within the time intervals from 0.3 to 0.8 seconds to fit in the line of best fit. Table 6.5 illustrates the overall gathered thermal conductivity values of the 4 different fluids at ambient temperature of 22°C.

Table 6.5. Measured thermal conductivity of fluids vs referenced values at 22°C

| Fluid | Measured thermal conductivity (W/mK) | Referenced thermal conductivity (W/mK) | Percent error (%) |
|--------------|---|---|--------------------------|
| Air | 0.0266 ± 0.0002 | 0.0259 [6] | 2.632 |
| IPA | 0.1425 ± 0.0031 | 0.1357 [47] | 4.772 |
| Ethanol | 0.1768 ± 0.0029 | 0.1698 [48] | 3.959 |
| DI Water | 0.6007 ± 0.0048 | 0.6014 [6] | 0.117 |

The customed designed apparatus is capable to extract thermal conductivity values from 0.026 W/mK to 0.73W/mK. The maximum value of 0.73 W/mK was obtained from the investigating the largest input current while utilizing the time range of 0.3 to 0.8 seconds with the wire's temperature rise of 0.27°C.

Chapter 7. Conclusion and Future Works

7.1. Conclusion

With a fully developed THW apparatus, the design can detect fluid's thermal conductivity. With air, IPA, ethanol, and DI water the required currents to detect their thermal conductivity is 20mA, 45mA, 50mA, and 95mA, respectively. With the experiment conducted for 10 seconds with 10 data sets obtained with the same parameter, the experimental error ranges from 0.117-4.772% indicating good agreement with the literature values of the measured fluids. It has been also found that the temperature rises to fit within the suggested time range of 0.3 to 0.8 seconds is found to be 0.27°C from the developed apparatus. With referencing known substance's thermophysical properties, using the same concept throughout the THW experiment to ensure the time ranges are fixed at 0.3 to 0.8 seconds and to have a temperature rise of at least 0.27°C by selecting the right input current will determine unknown fluid's thermal conductivity.

It has been also shown that the mathematical model of the THWM from investigating the literature works is a promising model to use when designing and implementing a different apparatus with specific dimensions. With the measurement time of the THWM kept short, this would illustrate consistent results of how the platinum wire would respond to the change in temperature from the joule heating effect. TPD and initial wire heating region must be investigated from the extracted data throughout the THW test. This is to ensure that data fits within the line of best fit as the platinum wire has a linear regression of the change in temperature with $\ln(t)$ for a short period of time.

From developing the THW test cell, calibrating the platinum wire to obtain its TCR would ensure that change in temperature is obtained from the voltage drop of the wire with the applied Heaviside step function. Insulation is vital for the platinum wire to not leak any electrical

current in the liquid medium as this would result to inconsistent joule heating to fulfil the THWM theory. The soldering technique used in this thesis required no special equipment to obtain the micro soldered joint. All the hands-on component integration was done by hand and utilized no special equipment for any precision engineering.

7.2. Future Works

With the extracted data of each fluid being tested at ambient temperature, it would be vital to measure fluids at different temperatures to ensure that the designed apparatus is capable to perform for hot and cold substances. With only fluids measured, the THW apparatus may have the potential to measure powders' thermal conductivity. As water has the highest thermal conductivity from the report of this thesis, a new designed cavity would expand the thermophysical property measurement range to measure thermally conductive fluids. With the current source ranging from 0-105mA, the platinum wire can be longer since resistance will also increase due to the resistivity equation and Ohm's Law to detect the necessary change in voltage for the measured material (that could contain a larger thermal conductivity value than water).

As the motivation behind this work is to characterize fluid's thermal conductivity from an experimental approach, the designed THWM can analyze unknown fluid's thermal conductivity values at short time durations. With the idea to enhance the HTF of a SWHS (mentioned earlier in the thesis) creating or altering the base fluid's thermophysical property can be investigated for future works. In order to enhance heat transfer, thermal conductivity must be increased which leads into the potential of creating nanofluids as they are known for their enhanced thermal conductivity values [14, 19, 20]. As Nanofluids thermal conductivity values are enhanced, the type of material, size, and shape do alter the heat transfer. To measure nanofluids, the designed THW test cell can be utilized to measure nanofluids with different volume fractions of

nanoparticles and surfactants to help stabilize the colloid solution. This opens to the next plan for future implementation and development for an enhanced SWHS.

References

- [1] R. Sahoo, P. Ghosh, and J. Sarkar, "Performance comparison of various coolants for louvered fin tube automotive radiator," *Therm. Sci.*, vol. 21, no. 6 Part B, pp. 2871–2881, 2017, doi: 10.2298/TSCI150219213S.
- [2] J. Borland and T. Tanaka, "Overcoming Barriers To 100% Clean Energy For Hawaii Starts At The Bottom Of The Energy Food Chain With Residential Island Nano-Grid And Everyday Lifestyle Behavioral Changes," in *2018 IEEE 7th World Conference on Photovoltaic Energy Conversion (WCPEC) (A Joint Conference of 45th IEEE PVSC, 28th PVSEC & 34th EU PVSEC)*, Waikoloa Village, HI, Jun. 2018, pp. 3829–3834. doi: 10.1109/PVSC.2018.8547382.
- [3] D. G. für Sonnenenergie, *Planning and Installing Solar Thermal Systems: A Guide for Installers, Architects and Engineers.*, Second. London: Earthscan, 2010.
- [4] T. W. Giambelluca *et al.*, "Solar Radiation of Hawai'i," *Evapotranspiration of Hawai'i.*, 2014. <http://evapotranspiration.geography.hawaii.edu/howtocite.html> (accessed Mar. 25, 2022).
- [5] G. Chen, *Nanoscale energy transport and conversion: a parallel treatment of electrons, molecules, phonons, and photons.* MASSACHUSETTS INSTITUTE OF TECHNOLOGY: Oxford university press, 2005.
- [6] T. Bergman, F. P. Incropera, D. P. DeWitt, and A. S. Lavine, *Fundamentals of heat and mass transfer*, 8th ed. John Wiley & Sons, 2011.
- [7] J. A. Eastman, S. R. Phillpot, S. U. S. Choi, and P. Keblinski, "THERMAL TRANSPORT IN NANOFLUIDS," *Annu. Rev. Mater. Res.*, vol. 34, no. 1, pp. 219–246, Aug. 2004, doi: 10.1146/annurev.matsci.34.052803.090621.
- [8] G. Xia, H. Jiang, R. Liu, and Y. Zhai, "Effects of surfactant on the stability and thermal conductivity of Al₂O₃/de-ionized water nanofluids," *Int. J. Therm. Sci.*, vol. 84, pp. 118–124, Oct. 2014, doi: 10.1016/j.ijthermalsci.2014.05.004.
- [9] S. Lee, S. U.-S. Choi, S. Li, and J. A. Eastman, "Measuring Thermal Conductivity of Fluids Containing Oxide Nanoparticles," *J. Heat Transf.*, vol. 121, no. 2, pp. 280–289, May 1999, doi: 10.1115/1.2825978.
- [10] N. Ali, J. A. Teixeira, and A. Addali, "A Review on Nanofluids: Fabrication, Stability, and Thermophysical Properties," *J. Nanomater.*, vol. 2018, pp. 1–33, Jun. 2018, doi: 10.1155/2018/6978130.
- [11] S. Almurtaji, N. Ali, J. A. Teixeira, and A. Addali, "On the Role of Nanofluids in Thermal-hydraulic Performance of Heat Exchangers—A Review," *Nanomaterials*, vol. 10, no. 4, p. 734, Apr. 2020, doi: 10.3390/nano10040734.
- [12] C. McAlinden, J. Khadka, and K. Pesudovs, "Precision (repeatability and reproducibility) studies and sample-size calculation," *J. Cataract Refract. Surg.*, vol. 41, no. 12, pp. 2598–2604, Dec. 2015, doi: 10.1016/j.jcrs.2015.06.029.
- [13] S. Singh, V. Sharma, and S. Narad, "Instruments to Measure Thermal Conductivity of Engineering Materials - A Brief Review," *J. Adv. Res. Mech. Eng. Technol.*, vol. 07, no. 1 & 2, pp. 16–25, Apr. 2020, doi: 10.24321/2454.8650.202001.
- [14] F. Guthrie, "I. On the thermal resistance of liquids," *Proc. R. Soc. Lond.*, vol. 17, pp. 233–236, Dec. 1869, doi: 10.1098/rspl.1868.0034.

- [15] S. Xu *et al.*, “Thermal properties of carbon nanofiber reinforced high-density polyethylene nanocomposites,” *J. Compos. Mater.*, vol. 49, no. 7, pp. 795–805, Mar. 2015, doi: 10.1177/0021998314525980.
- [16] M. Akoshima and T. Baba, “Study on a Thermal-diffusivity Standard for Laser Flash Method Measurements,” *Int. J. Thermophys.*, vol. 27, no. 4, pp. 1189–1203, Jul. 2006, doi: 10.1007/s10765-006-0091-9.
- [17] W. J. Parker, R. J. Jenkins, C. P. Butler, and G. L. Abbott, “Flash Method of Determining Thermal Diffusivity, Heat Capacity, and Thermal Conductivity,” *J. Appl. Phys.*, vol. 32, no. 9, pp. 1679–1684, Sep. 1961, doi: 10.1063/1.1728417.
- [18] S. Krenek, K. Anhalt, A. Lindemann, C. Monte, J. Hollandt, and J. Hartmann, “A Study on the Feasibility of Measuring the Emissivity with the Laser-Flash Method,” *Int. J. Thermophys.*, vol. 31, no. 4–5, pp. 998–1010, May 2010, doi: 10.1007/s10765-010-0767-z.
- [19] Y. Tada, M. Harada, M. Tanigaki, and W. Eguchi, “Laser flash method for measuring thermal conductivity of liquids—application to low thermal conductivity liquids,” *Rev. Sci. Instrum.*, vol. 49, no. 9, pp. 1305–1314, Sep. 1978, doi: 10.1063/1.1135573.
- [20] T. T. Loong and H. Salleh, “A review on measurement techniques of apparent thermal conductivity of nanofluids,” Aug. 2017, vol. 226, p. 012146. doi: 10.1088/1757-899X/226/1/012146.
- [21] S. A. Al-Ajlan, “Measurements of thermal properties of insulation materials by using transient plane source technique,” *Appl. Therm. Eng.*, vol. 26, no. 17–18, pp. 2184–2191, Dec. 2006, doi: 10.1016/j.applthermaleng.2006.04.006.
- [22] T. Log and S. E. Gustafsson, “Transient plane source (TPS) technique for measuring thermal transport properties of building materials,” *Fire Mater.*, vol. 19, no. 1, pp. 43–49, Jan. 1995, doi: 10.1002/fam.810190107.
- [23] X. Yan, “On the Penetration Depth in Fourier Heat Conduction,” presented at the 8th AIAA/ASME Joint Thermophysics and Heat Transfer Conference, St. Louis, Missouri, Jun. 2002. doi: 10.2514/6.2002-2881.
- [24] Y. Li *et al.*, “Improving the accuracy of the transient plane source method by correcting probe heat capacity and resistance influences,” *Meas. Sci. Technol.*, vol. 25, no. 1, p. 015006, Jan. 2014, doi: 10.1088/0957-0233/25/1/015006.
- [25] R. A. Perkins, H. M. Roder, and C. A. N. Decastro, “A high-temperature transient hot-wire thermal conductivity apparatus for fluids,” *J. Res. Natl. Inst. Stand. Technol.*, vol. 96, no. 3, p. 247, May 1991, doi: 10.6028/jres.096.014.
- [26] H. S. Carslaw and J. C. Jaeger, *Conduction of heat in solids*, Second. Oxford at the Clarendon Press, 1959.
- [27] D. Yoo, J. Lee, B. Lee, S. Kwon, and J. Koo, “Further elucidation of nanofluid thermal conductivity measurement using a transient hot-wire method apparatus,” *Heat Mass Transf.*, vol. 54, no. 2, pp. 415–424, Feb. 2018, doi: 10.1007/s00231-017-2144-y.
- [28] L. C. Wei, L. E. Ehrlich, M. J. Powell-Palm, C. Montgomery, J. Beuth, and J. A. Malen, “Thermal conductivity of metal powders for powder bed additive manufacturing,” *Addit. Manuf.*, vol. 21, pp. 201–208, May 2018, doi: 10.1016/j.addma.2018.02.002.
- [29] B. Merckx, P. Dudoignon, J. P. Garnier, and D. Marchand, “Simplified Transient Hot-Wire Method for Effective Thermal Conductivity Measurement in Geo Materials: Microstructure and Saturation Effect,” *Adv. Civ. Eng.*, vol. 2012, pp. 1–10, 2012, doi: 10.1155/2012/625395.

- [30] J. J. Ma, “Thermal Conductivity of Fluids Containing Suspension of Nanometer-Sized Particles,” MASSACHUSETTS INSTITUTE OF TECHNOLOGY, 2006. [Online]. Available: <http://dspace.mit.edu/handle/1721.1/7582>
- [31] L. E. Ehrlich, J. S. G. Feig, S. N. Schiffres, J. A. Malen, and Y. Rabin, “Large Thermal Conductivity Differences between the Crystalline and Vitrified States of DMSO with Applications to Cryopreservation,” *PLOS ONE*, vol. 10, no. 5, p. e0125862, May 2015, doi: 10.1371/journal.pone.0125862.
- [32] Y. Nagasaka and A. Nagashima, “Absolute measurement of the thermal conductivity of electrically conducting liquids by the transient hot-wire method,” *J. Phys. [E]*, vol. 14, no. 12, pp. 1435–1440, Dec. 1981, doi: 10.1088/0022-3735/14/12/020.
- [33] H. M. Roder, “A Transient Hot Wire Thermal Conductivity Apparatus for Fluids,” *J. Res. Natl. Bur. Stand.*, vol. 86, no. 5, p. 457, Sep. 1981, doi: 10.6028/jres.086.020.
- [34] J. J. Healy, J. J. de Groot, and J. Kestin, “The theory of the transient hot-wire method for measuring thermal conductivity,” *Phys. BC*, vol. 82, no. 2, pp. 392–408, Apr. 1976, doi: 10.1016/0378-4363(76)90203-5.
- [35] J. J. De Groot, J. Kestin, and H. Sookiazian, “Instrument to measure the thermal conductivity of gases,” *Physica*, vol. 75, no. 3, pp. 454–482, Aug. 1974, doi: 10.1016/0031-8914(74)90341-3.
- [36] J. W. Haarman, “A contribution to the theory of the transient hot-wire method,” *Physica*, vol. 52, no. 4, pp. 605–619, Apr. 1971, doi: 10.1016/0031-8914(71)90165-0.
- [37] P. G. Knibbe, “The end-effect error in the determination of thermal conductivity using a hot-wire apparatus,” *Int. J. Heat Mass Transf.*, vol. 29, no. 3, pp. 463–473, Mar. 1986, doi: 10.1016/0017-9310(86)90215-2.
- [38] “Transient-Hot-Wire method for determining thermal conductivity (THW),” *Tec-Science*, 2022. <https://www.tec-science.com/thermodynamics/heat/transient-hot-wire-method-method-for-determining-thermal-conductivity-thw/>
- [39] S. Maki *et al.*, “Temperature Dependence and Anisotropic Effects in the Thermal Properties of Hen Egg-White Lysozyme Crystals,” *Symmetry*, vol. 12, no. 8, p. 1279, Aug. 2020, doi: 10.3390/sym12081279.
- [40] S. W. Hong, Y. T. Kang, C. Kleinstreuer, and J. Koo, “Impact analysis of natural convection on thermal conductivity measurements of nanofluids using the transient hot-wire method,” *Int. J. Heat Mass Transf.*, vol. 54, no. 15–16, pp. 3448–3456, Jul. 2011, doi: <https://doi.org/10.1016/j.ijheatmasstransfer.2011.03.041>.
- [41] S. W. Hong, J.-Y. Jung, Y. T. Kang, and J. Koo, “PARAMETRIC STUDY ON TRANSIENT HOT-WIRE METHOD TO MEASURE NANOFLUID CONDUCTIVITIES,” *Int. J. Air-Cond. Refrig.*, vol. 18, no. 03, pp. 191–199, Sep. 2010, doi: 10.1142/S2010132510000186.
- [42] “American Wire Gauge Conversion Chart | AWG Sizes,” *Rembar Co.* <https://www.rembar.com/resources-technical-information-on-refractory-metals/american-wire-gauge-awg/> (accessed Mar. 21, 2022).
- [43] L. Abadlia, F. Gasser, K. Khalouk, M. Mayoufi, and J. G. Gasser, “New experimental methodology, setup and LabView program for accurate absolute thermoelectric power and electrical resistivity measurements between 25 and 1600 K: Application to pure copper, platinum, tungsten, and nickel at very high temperatures,” *Rev. Sci. Instrum.*, vol. 85, no. 9, p. 095121, Sep. 2014, doi: 10.1063/1.4896046.

- [44] E. G. Price and B. Taylor, "Temperature Coefficient of Electrical Resistance of High-Purity Rhodium," *Nature*, vol. 195, no. 4838, pp. 272–273, Jul. 1962, doi: 10.1038/195272a0.
- [45] D. K. Lee, J. In, and S. Lee, "Standard deviation and standard error of the mean," *Korean J. Anesthesiol.*, vol. 68, no. 3, p. 220, 2015, doi: 10.4097/kjae.2015.68.3.220.
- [46] K. Stephan and A. Laesecke, "The Thermal Conductivity of Fluid Air," *J. Phys. Chem. Ref. Data*, vol. 14, no. 1, pp. 227–234, Jan. 1985, doi: 10.1063/1.555749.
- [47] "Isopropyl Alcohol's Thermophysical Properties."
<https://www.google.com/url?sa=t&rct=j&q=&esrc=s&source=web&cd=&ved=2ahUKewjpxs31uYv3AhUgJzQIHZaaAY8QFnoECCIQAQ&url=https%3A%2F%2Fcameochemicals.noaa.gov%2Fchris%2FIPA.pdf&usg=AOvVaw22XEcQwrLiHKBgBFyYGVk1> (accessed Mar. 31, 2022).
- [48] J. Petracic, "Thermal conductivity of ethanol," *J. Chem. Phys.*, vol. 123, no. 17, p. 174503, Nov. 2005, doi: 10.1063/1.2102867.
- [49] J. V. Sengers and J. T. R. Watson, "Improved International Formulations for the Viscosity and Thermal Conductivity of Water Substance," *J. Phys. Chem. Ref. Data*, vol. 15, no. 4, pp. 1291–1314, Oct. 1986, doi: 10.1063/1.555763.

Appendices

Appendix A: Thermophysical properties of conventional fluids

Table A.1. Water's thermophysical properties at atmospheric pressure [6]

| Temperature (T) [°C] | Density (ρ) [kg/m ³] | Dynamic Viscosity (μ) [Pa.s] | Kinematic Viscosity (ν) [m ² /s] | Specific Heat Capacity (Cp) [J/kg.K] | Thermal Conductivity (k) [W/m.K] | Prandtl Number (Pr) | Thermal diffusivity (α) [m ² /s] |
|-------------------------|---|--|---|--|--|---------------------------|--|
| $\times 10^0$ | $\times 10^0$ | $\times 10^{-3}$ | $\times 10^{-6}$ | $\times 10^0$ | $\times 10^0$ | $\times 10^0$ | $\times 10^{-7}$ |
| 0 | 999.84 | 1.792 | 1.792 | 4219.0 | 0.561 | 13.47 | 1.330 |
| 5 | 999.97 | 1.518 | 1.518 | 4216.2 | 0.571 | 11.19 | 1.358 |
| 10 | 999.70 | 1.306 | 1.306 | 4213.4 | 0.580 | 9.45 | 1.383 |
| 15 | 999.10 | 1.138 | 1.139 | 4210.6 | 0.589 | 8.09 | 1.407 |
| 20 | 998.21 | 1.002 | 1.003 | 4207.8 | 0.598 | 7.00 | 1.432 |
| 25 | 997.05 | 0.890 | 0.893 | 4205.0 | 0.607 | 6.13 | 1.456 |
| 30 | 995.65 | 0.797 | 0.801 | 4203.0 | 0.616 | 5.41 | 1.480 |
| 35 | 994.04 | 0.719 | 0.724 | 4201.0 | 0.623 | 4.82 | 1.499 |
| 40 | 992.22 | 0.653 | 0.658 | 4199.0 | 0.631 | 4.33 | 1.522 |
| 45 | 990.22 | 0.596 | 0.602 | 4197.0 | 0.637 | 3.91 | 1.539 |
| 50 | 988.05 | 0.547 | 0.553 | 4195.0 | 0.644 | 3.55 | 1.559 |
| 55 | 985.71 | 0.504 | 0.511 | 4193.8 | 0.649 | 3.25 | 1.575 |
| 60 | 983.21 | 0.466 | 0.474 | 4192.6 | 0.654 | 2.98 | 1.590 |
| 65 | 980.57 | 0.433 | 0.442 | 4191.4 | 0.659 | 2.75 | 1.606 |
| 70 | 977.78 | 0.404 | 0.413 | 4190.2 | 0.663 | 2.55 | 1.619 |
| 75 | 974.86 | 0.378 | 0.387 | 4189.0 | 0.667 | 2.37 | 1.632 |
| 80 | 971.80 | 0.354 | 0.365 | 4188.2 | 0.670 | 2.22 | 1.643 |
| 85 | 968.62 | 0.333 | 0.344 | 4187.4 | 0.673 | 2.08 | 1.654 |
| 90 | 965.32 | 0.314 | 0.326 | 4186.6 | 0.675 | 1.96 | 1.663 |
| 95 | 961.90 | 0.297 | 0.309 | 4185.8 | 0.677 | 1.85 | 1.671 |
| 100 | 958.43 | 0.282 | 0.294 | 4185.0 | 0.679 | 1.75 | 1.680 |

Table A.2. Thermophysical properties of air at atmospheric pressure [6]

| Temperature (T) [°C] | Density (ρ) [kg/m ³] | Dynamic Viscosity (μ) [Pa.s] | Kinematic Viscosity (ν) [m ² /s] | Specific Heat Capacity (C _p) [J/kg.K] | Thermal Conductivity (k) [W/m.K] | Prandtl Number (Pr) | Thermal diffusivity (α) [m ² /s] |
|-------------------------|---|--|---|---|--|---------------------------|--|
| x10 ⁰ | x10 ⁰ | x10 ⁻⁷ | x10 ⁻⁶ | x10 ⁰ | x10 ⁰ | x10 ⁰ | x10 ⁻⁶ |
| 0 | 1.287 | 159.60 | 13.49 | 1006.5 | 0.0241 | 0.720 | 15.89 |
| 1 | 1.283 | 160.10 | 13.58 | 1006.5 | 0.0242 | 0.720 | 16.00 |
| 2 | 1.278 | 160.60 | 13.67 | 1006.5 | 0.0243 | 0.721 | 16.11 |
| 3 | 1.273 | 161.10 | 13.75 | 1006.5 | 0.0244 | 0.721 | 16.23 |
| 4 | 1.269 | 161.60 | 13.84 | 1006.5 | 0.0245 | 0.722 | 16.34 |
| 5 | 1.264 | 162.10 | 13.93 | 1006.6 | 0.0245 | 0.722 | 16.45 |
| 6 | 1.259 | 162.60 | 14.02 | 1006.6 | 0.0246 | 0.723 | 16.57 |
| 7 | 1.255 | 163.10 | 14.11 | 1006.6 | 0.0247 | 0.723 | 16.68 |
| 8 | 1.250 | 163.60 | 14.20 | 1006.6 | 0.0248 | 0.723 | 16.80 |
| 9 | 1.245 | 164.10 | 14.29 | 1006.6 | 0.0249 | 0.724 | 16.91 |
| 10 | 1.241 | 164.60 | 14.38 | 1006.7 | 0.0249 | 0.724 | 17.03 |
| 11 | 1.236 | 165.10 | 14.47 | 1006.7 | 0.0250 | 0.724 | 17.15 |
| 12 | 1.231 | 165.60 | 14.56 | 1006.7 | 0.0251 | 0.724 | 17.27 |
| 13 | 1.227 | 166.10 | 14.64 | 1006.7 | 0.0252 | 0.725 | 17.39 |
| 14 | 1.222 | 166.60 | 14.73 | 1006.7 | 0.0253 | 0.725 | 17.51 |
| 15 | 1.217 | 167.10 | 14.82 | 1006.8 | 0.0253 | 0.725 | 17.63 |
| 16 | 1.213 | 167.60 | 14.91 | 1006.8 | 0.0254 | 0.725 | 17.75 |
| 17 | 1.208 | 168.10 | 15.00 | 1006.8 | 0.0255 | 0.725 | 17.87 |
| 18 | 1.203 | 168.60 | 15.09 | 1006.8 | 0.0256 | 0.725 | 18.00 |
| 19 | 1.199 | 169.10 | 15.18 | 1006.8 | 0.0257 | 0.725 | 18.12 |
| 20 | 1.194 | 169.60 | 15.27 | 1006.9 | 0.0257 | 0.724 | 18.25 |
| 21 | 1.189 | 170.10 | 15.36 | 1006.9 | 0.0258 | 0.724 | 18.37 |
| 22 | 1.185 | 170.60 | 15.45 | 1006.9 | 0.0259 | 0.724 | 18.50 |
| 23 | 1.180 | 171.10 | 15.53 | 1006.9 | 0.0260 | 0.724 | 18.63 |
| 24 | 1.175 | 171.60 | 15.62 | 1006.9 | 0.0261 | 0.724 | 18.76 |
| 25 | 1.171 | 172.10 | 15.71 | 1007.0 | 0.0261 | 0.723 | 18.89 |
| 26 | 1.166 | 172.60 | 15.80 | 1007.0 | 0.0262 | 0.723 | 19.02 |
| 27 | 1.161 | 173.10 | 15.89 | 1007.0 | 0.0263 | 0.723 | 19.15 |
| 28 | 1.158 | 173.60 | 15.99 | 1007.0 | 0.0264 | 0.722 | 19.29 |
| 29 | 1.155 | 174.10 | 16.09 | 1007.1 | 0.0264 | 0.722 | 19.42 |
| 30 | 1.151 | 174.60 | 16.19 | 1007.1 | 0.0265 | 0.721 | 19.56 |

Table A.3. Thermophysical properties of ethylene glycol at atmospheric pressure [6]

| Temperature (T) [°C] | Density (ρ) [kg/m ³] | Dynamic Viscosity (μ) [Pa.s] | Kinematic Viscosity (ν) [m ² /s] | Specific Heat Capacity (Cp) [J/kg.K] | Thermal Conductivity (k) [W/m.K] | Prandtl Number (Pr) | Thermal diffusivity (α) [m ² /s] |
|-------------------------|--|--|---|--|--|---------------------------|--|
| $\times 10^0$ | $\times 10^0$ | $\times 10^{-7}$ | $\times 10^{-6}$ | $\times 10^0$ | $\times 10^0$ | $\times 10^0$ | $\times 10^{-6}$ |
| 0 | 1130.8 | 6.51 | 57.60 | 2294.0 | 0.242 | 617.4 | 9.329 |
| 5 | 1127.2 | 4.86 | 43.10 | 2314.7 | 0.243 | 462.0 | 9.330 |
| 10 | 1123.7 | 3.68 | 32.74 | 2336.5 | 0.245 | 350.6 | 9.339 |
| 15 | 1120.2 | 2.82 | 25.14 | 2359.0 | 0.247 | 268.7 | 9.355 |
| 20 | 1117.5 | 2.20 | 19.70 | 2382.1 | 0.249 | 210.4 | 9.362 |
| 25 | 1115.3 | 1.75 | 15.70 | 2405.6 | 0.251 | 167.7 | 9.363 |
| 30 | 1111.2 | 1.42 | 12.77 | 2428.5 | 0.253 | 136.2 | 9.372 |
| 35 | 1105.8 | 1.17 | 10.54 | 2451.0 | 0.254 | 112.3 | 9.386 |
| 40 | 1101.5 | 0.98 | 8.83 | 2473.5 | 0.256 | 94.0 | 9.393 |
| 45 | 1097.7 | 0.82 | 7.46 | 2496.0 | 0.257 | 79.4 | 9.395 |
| 50 | 1094.2 | 0.70 | 6.38 | 2518.2 | 0.259 | 68.0 | 9.385 |
| 55 | 1090.8 | 0.60 | 5.50 | 2540.2 | 0.260 | 58.7 | 9.369 |
| 60 | 1087.8 | 0.52 | 4.80 | 2561.9 | 0.260 | 51.4 | 9.340 |
| 65 | 1084.9 | 0.46 | 4.21 | 2583.4 | 0.261 | 45.3 | 9.305 |
| 70 | 1082.4 | 0.40 | 3.74 | 2605.5 | 0.261 | 40.4 | 9.255 |
| 75 | 1080.0 | 0.36 | 3.33 | 2628.0 | 0.261 | 36.2 | 9.196 |
| 80 | 1077.5 | 0.32 | 3.00 | 2650.5 | 0.261 | 32.8 | 9.139 |
| 85 | 1075.0 | 0.29 | 2.71 | 2673.0 | 0.261 | 29.8 | 9.083 |
| 90 | 1071.8 | 0.26 | 2.46 | 2695.8 | 0.261 | 27.1 | 9.043 |
| 95 | 1068.2 | 0.24 | 2.23 | 2718.8 | 0.262 | 24.7 | 9.015 |
| 100 | 1058.5 | 0.22 | 2.03 | 2742.0 | 0.263 | 22.4 | 9.061 |

Table A.4. Ethanol's thermal conductivity at different temperatures [48]

| Temperature (T) [°C] | Thermal Conductivity (k) [W/m.K] |
|---------------------------------|---|
| 0 | 0.1724 |
| 5 | 0.1712 |
| 10 | 0.1700 |
| 15 | 0.1689 |
| 20 | 0.1678 |
| 21 | 0.1676 |
| 22 | 0.1674 |
| 23 | 0.1671 |
| 24 | 0.1669 |
| 25 | 0.1667 |
| 26 | 0.1664 |
| 27 | 0.1662 |
| 28 | 0.1659 |
| 29 | 0.1657 |
| 30 | 0.1655 |

Table A.5 Isopropyl alcohol's thermal conductivity at different temperatures [47]

| Temperature (T) [°C] | Thermal Conductivity (k) [W/m.K] |
|-------------------------|--|
| 10 | 0.1371 |
| 11 | 0.1369 |
| 12 | 0.1368 |
| 13 | 0.1366 |
| 14 | 0.1364 |
| 15 | 0.1362 |
| 16 | 0.1360 |
| 17 | 0.1358 |
| 18 | 0.1356 |
| 19 | 0.1354 |
| 20 | 0.1352 |
| 21 | 0.1350 |
| 22 | 0.1347 |
| 23 | 0.1345 |
| 24 | 0.1343 |
| 25 | 0.1341 |
| 26 | 0.1339 |
| 27 | 0.1337 |
| 28 | 0.1335 |

Appendix B: MATLAB Codes utilized

B.1 Raw data extraction data (from THW setup)

```
%%
%Setup for MCC DAQ system
d = daqlist("mcc"); %Verification that DAQ system is detected
d(1, :)

dq = daq("mcc") %Generating a recording session

%Adding the CH0 input for detection circuitry. Ensure CH0 differential mode
%is connected to CH0 HI, LO, and GND
addinput(dq, "Board0", "Ai0", "Voltage");

%Verification and setup for the Kiethley 6221 System
%WIP for generating obj1 automatically
obj1

fprintf(obj1, '*IDN?')
fscanf(obj1)

%%
%Set up desired sample rate
%Note: Will sample this many times over the time period dictated in
%recording actuation code
dq.Rate = 1000
ch0.Range=[-10,10]

%% Linear Sweep Activation

fprintf(obj1, 'SOUR:CURREN 0e-3')
fprintf(obj1, 'SOUR:CURREN:COMP 10')
fprintf(obj1, 'SOUR:CURREN:STAR 20e-3') %% Start value for our Linear Step
fprintf(obj1, 'SOUR:CURREN:STOP 20e-3') %% Stop value for our Linear Step
fprintf(obj1, 'SOUR:DEL 1') %% Delay between steps
fprintf(obj1, 'SOUR:SWE:COUN 1')
fprintf(obj1, 'SOUR:SWE:CAB OFF')
fprintf(obj1, 'SOUR:SWE:ARM')
%%
fprintf(obj1, 'INIT') %% Initialize armed waveform
%Start recording of DAQ
[data, startTime] = read(dq, seconds(10));
pause(2)
fprintf(obj1, 'OUTP OFF') %% Secures waveform reading
%%

figure(1)
scatter(data.Time, data.Board0_Ai0);
xlabel("Time (s)");
ylabel("Voltage (V)");
title('Experimental Voltage');
grid on;
grid minor;
```

```

writematrix(data.Time, 'datatimeRAW.csv');
writematrix(data.Board0_Ai0, 'datavoltRAW_gain_HDR.csv'); %--change mA and
gain--%
GAIN= 20; % Physically refer to the voltage amplifier %--change mA and gain--%
%

ConvertVOLT=data.Board0_Ai0/GAIN;
writematrix(ConvertVOLT,'datavoltAMP_gain_HDR.csv'); %--change mA and gain--%

% Helps to readtable to extract the data than using Excel
data_t = readtable('datatimeRAW.csv');
data_V = readtable('datavoltAMP_gain_HDR.csv'); %--change mA and gain--%

```

B.2 Averaging extracted data MATLAB code

```

t= 0:0.001:0.9999; %change the time limits when possible (other data might be
different)
% Reads the data from csv
data1 =
xlsread('20220114_Convert_Water_GAIN5_105mA_1000samples_1sec_LONGcavity_22Deg
_T1.csv'); % two columns of data
data2 =
xlsread('20220114_Convert_Water_GAIN5_105mA_1000samples_1sec_LONGcavity_22Deg
_T2.csv'); % two columns of data
data3 =
xlsread('20220114_Convert_Water_GAIN5_105mA_1000samples_1sec_LONGcavity_22Deg
_T3.csv'); % two columns of data
data4 =
xlsread('20220114_Convert_Water_GAIN5_105mA_1000samples_1sec_LONGcavity_22Deg
_T4.csv'); % two columns of data
data5 =
xlsread('20220114_Convert_Water_GAIN5_105mA_1000samples_1sec_LONGcavity_22Deg
_T5.csv'); % two columns of data
data6 =
xlsread('20220114_Convert_Water_GAIN5_105mA_1000samples_1sec_LONGcavity_22Deg
_T6.csv'); % two columns of data
data7 =
xlsread('20220114_Convert_Water_GAIN5_105mA_1000samples_1sec_LONGcavity_22Deg
_T7.csv'); % two columns of data
data8 =
xlsread('20220114_Convert_Water_GAIN5_105mA_1000samples_1sec_LONGcavity_22Deg
_T8.csv'); % two columns of data
data9 =
xlsread('20220114_Convert_Water_GAIN5_105mA_1000samples_1sec_LONGcavity_22Deg
_T9.csv'); % two columns of data
data10 =
xlsread('20220114_Convert_Water_GAIN5_105mA_1000samples_1sec_LONGcavity_22Deg
_T10.csv'); % two columns of data

% averages the data out for each file
a1= mean(data1,2);
a2= mean(data2,2);

```

```

a3= mean(data3,2);
a4= mean(data4,2);
a5= mean(data5,2);
a6= mean(data6,2);
a7= mean(data7,2);
a8= mean(data8,2);
a9= mean(data9,2);
a10= mean(data10,2);
Average_V=(a1+a2+a3+a4+a5+a6+a7+a8+a9+a10)/10;
S = std(Average_V)
STDM= S/sqrt(10)
% extracts the average values and convert to csv
writematrix(Average_V, '20220114_Convert_Water_GAIN5_105mA_1000samples_1sec_LO
NGcavity_22Deg_AVERAGE.csv');

```

B.3 Code to initiate thermal conductivity measurement

```

%% Analyze converted voltages to Thermal conductivity OLD technique
clc;
%-----initial important parameters (INPUT HERE)-----
-----%
Current = 0.045; % mA to Amperes
Wire_Length= 38.5 ;%39 ; % units in mm please
Temperature_Fluid= 22 ; %temperature of fluid From data file name

time1= 0.3 ;
time2= 0.8 ;

TimeRange= log(time2/time1);

data_t = readtable('datatimeRAW_1000hz_10sec.csv');
data_V =
readtable('20220328_Convert_IPA_GAIN5_45mA_1000samples_10sec_SHORTcavity_20De
g_COVER_12db_20v_100NEW_AVERAGE.csv');

% Reads the first row from the raw time values taken from DAQ
data_t = (data_t.Var1);

% Change in voltage values
data_V = table2array(data_V);
x=data_t;
Volts=data_V;

I=Current; % current going into wire
current=I*1000; %input at the end of the fprintf section
t1=log(data_t); % natural log of time
Resistance=(Volts)/I ;% resistance **** GRAPH PORTION*****
%V_0= Volts(1);
writematrix(Resistance, 'Resistance.csv');

R_0= 8.7 ;% Reference Resistance at temperature of 22 degrees Celsius

TCR_Slope = 0.03181 ; %TCR of the slope from the calibration graph

```

```

TCR= TCR_Slope/ R_0 ;%0.003520; % temperature coefficient of resistance
L=Wire_Length*10^-3; % converts to m LENGTH OF WIRE
Q=(R_0)*I^2 ; % heat input to the platinum wire
Constant = Q/(4*pi*L); % the q' over 4pi initial value

% Converted voltage transient graph
figure(1)
scatter(data_t,Volts,45,'MarkerEdgeColor','k', 'MarkerFaceColor',[1 0.89
0.4]);
hold on
xlabel('Time (s)','FontSize', 15, 'FontWeight', 'bold')
ylabel('Converted Change in Volts (?V)','FontSize', 15, 'FontWeight',
'bold')
title('Voltage Drop of Wire over Time','FontSize', 15, 'FontWeight',
'bold');
grid on;
grid minor;
legend('Voltages','location', 'southeast');
hold off;

% TEMPERATURE DATA TO EXCEL FILE

Temp1= (Resistance-R_0)/(TCR_Slope) ;
writematrix(Volts,'Voltage_Values.csv');
writematrix(Temp1,'Temperature1.csv');

figure(2) % RESSITANCE GRAPH
scatter(data_t, Resistance,45,'MarkerEdgeColor','k', 'MarkerFaceColor',[0
0.5 0.8]);
hold on;
xlabel("Time (s)","FontSize", 15, 'FontWeight', 'bold');
ylabel("Change in Resistance (?R)","FontSize", 15, 'FontWeight', 'bold');
title("Change in Wire's Resistance","FontSize", 15, 'FontWeight',
'bold');
grid on;
grid minor;
legend('Resistance','location', 'southeast');
hold off;

figure(3) % TEMPERATURE GRAPH
scatter(data_t,Temp1,45,'MarkerEdgeColor','k', 'MarkerFaceColor',[1 0
0]);
hold on
xlabel('Time (s)','FontSize', 15, 'FontWeight', 'bold')
ylabel('Temperature of Wire (?K)','FontSize', 15, 'FontWeight', 'bold')
title('Change in Temperature of Wire','FontSize', 15, 'FontWeight',
'bold');
grid on;
grid minor;
legend('Temperature','location','southeast');
hold off;

% technique 1 to extract thermal conductivity of fluids

```

```

figure(4) % TEMPERATURE log scale time
scatter(data_t, Temp,45,'MarkerEdgeColor','k', 'MarkerFaceColor',[1 0
0]);
set(gca,'xscale','log')
xlabel("Time (s)",'FontSize', 15, 'FontWeight', 'bold');
ylabel("Temperature of Wire (?K)",'FontSize', 15, 'FontWeight', 'bold');
title('Change in Temperature of Wire','FontSize', 15, 'FontWeight',
'bold');
grid on;
grid minor;
legend('Temperature','location', 'southeast');
hold off;

figure(5) % TEMPERATURE VS NATURAL LOG TIME GRAPH
scatter(t1, Temp1,45,'MarkerEdgeColor','k', 'MarkerFaceColor',[0 1 0]);
xlabel("ln(t)",'FontSize', 15, 'FontWeight', 'bold');
ylabel("Temperature of Wire (?K)",'FontSize', 15, 'FontWeight', 'bold');
title('Temperature of Wire over time','FontSize', 15, 'FontWeight',
'bold');
grid on;
grid minor;
legend('Temperature','location', 'southeast');
ind = t1>=log(time1) & t1<=log(time2);
p = polyfit(t1(ind),Temp1(ind),1) ;
slope1 = p(1);
intercept = p(2);
f = polyval(p,t1(ind));
hold on;
plot(t1(ind),f,'-','LineWidth',2.5,'Color',[1 0 0]) ;
legend('Temperature','Linear fit');
SStot = sum((Temp1-mean(Temp1(ind))).^2); % Total Sum-Of-Squares
SSres = sum((Temp1(ind)-f).^2); % Residual Sum-Of-Squares
Rsq_1 = 1-SSres/SStot ; % R^2 value
hold off;

csv1 = csvread('Voltage_Values.csv');
csv2 = csvread('Temperature.csv');
all_CSV = [csv1 csv2 ];
writematrix(all_CSV,'Voltage_Temperature.csv');

DATA_USE= readtable('Voltage_Temperature.csv');
data=table2array(DATA_USE);

m= zeros(10000, 1); %initialize m array
for n = 1: length(m)
    THWM(n,1)=(4*pi*(data(n,2)))/(I*(data(n,1))/L); %Iteratively computes m
end

figure(6)
scatter(data_t, THWM,45,'MarkerEdgeColor','k', 'MarkerFaceColor',[1 0.5
0]);
xlabel("Time (s)",'FontSize', 15, 'FontWeight', 'bold');
ylabel("4πT/q' (W^-^1mK)",'FontSize', 15, 'FontWeight', 'bold');
title('Thermal Conductivity Extraction','FontSize', 18, 'FontWeight',
'bold');

```

```

grid on;
grid minor;
legend('Thermal Conductivity Extraction','location', 'southeast');
hold off;

figure(7)
scatter(t1, THWM,45,'MarkerEdgeColor','k', 'MarkerFaceColor',[0 0.4
0.9]);
xlabel("ln(t)", 'FontSize', 15, 'FontWeight', 'bold');
ylabel("4??T/q' (W^-^1mK)", 'FontSize', 15, 'FontWeight', 'bold');
title('Thermal Conductivity Extraction', 'FontSize', 18, 'FontWeight',
'bold');
grid on;
grid minor;
legend('Thermal Conductivity Extraction','location', 'southeast');
hold on;

%-----%
ind = t1>=log(time1) & t1<=log(time2);
%-----%
p = polyfit(t1(ind),THWM(ind),1) ;
slope2 = p(1);
intercept = p(2);
f = polyval(p,t1(ind));
hold on;
plot(t1(ind),f, '-','LineWidth',2.5,'Color',[1 0 0]) ;
legend('Thermal Conductivity Extraction','Linear fit');
SStot = sum((THWM-mean(THWM(ind))).^2); % Total Sum-Of-Squares
SSres = sum((THWM(ind)-f).^2); % Residual Sum-Of-Squares
Rsq_2 = 1-SSres/SStot ; % R^2 value
hold off;

k2=(1/slope2); %technique #2
k1= Constant*(1/slope1); % thermal conductivity extraction Technique #1

%----- Referenced fluid's thermal conductivity %Error ----
%-----%

% Refernce thermal condcutivity of water and Air
k_ref_WATER=0.6014; % at 22°C for water W/mK
k_ref_AIR=0.026; % at 22°C for air W/mK
k_ref_IPA=0.1357; % at 22°C for air W/mK
k_ref_Ethanol = 0.1698 ; % at 22°C for ethanol W/mK

%Percent_error1= (abs(k1-k_ref_WATER)/k1)*100; % technique 1
%Percent_error1= (abs(k1-k_ref_AIR)/k1)*100 ; % technique 1
Percent_error1= (abs(k1-k_ref_IPA)/k1)*100 ; % technique 1
%Percent_error1= (abs(k1-k_ref_Ethanol)/k1)*100 ; % technique 1

%Percent_error2= (abs(k2-k_ref_WATER)/k2)*100; % technique 2
%Percent_error2= (abs(k2-k_ref_AIR)/k2)*100 ; % technique 2
Percent_error2= (abs(k2-k_ref_IPA)/k2)*100 ; % technique 2
%Percent_error2= (abs(k2-k_ref_Ethanol)/k2)*100 ; % technique 2

Change_Temp= slope1*(log(time2/time1)); % change in temperature

```

```

fprintf("Initial resistance is %0.4f Ohms.\n",R_0)
fprintf("Heat input is %0.4f Watts.\n",Q)
fprintf("Current of %0.1f mA.\n",current)
fprintf("The q'/4? is %0.4f W/m.\n",Constant)
fprintf("The time range of ln(0.8/0.3) is %0.4f.\n",TimeRange)
fprintf("The slope of ?T/ln(t) is %0.4f K.\n",slope1)
fprintf("The Change in temperature range is %0.4f K.\n",Change_Temp)

% Air %
% fprintf("Air's thermal conductivity at %1.1f°C is %0.4f W/mK technique #1,
percent error is %0.4f%%.\n", Temperature_Fluid, k1, Percent_error1);
% fprintf("Air's thermal conductivity at %1.1f°C is %0.4f W/mK technique #2,
percent error is %0.4f%%.\n", Temperature_Fluid, k2, Percent_error2);
% fprintf("Air's thermal conductivity from reference is %0.4f W/mK at
%1.1f°C. \n", k_ref_AIR, Temperature_Fluid);

% Water %
%fprintf("Water's thermal conductivity at %1.1f°C is %0.4f W/mK technique #1,
percent error is %0.4f%%.\n",Temperature_Fluid, k1, Percent_error1);
%fprintf("Water's thermal conductivity at %1.1f°C is %0.4f W/mK technique #2,
percent error is %0.4f%%.\n",Temperature_Fluid, k2, Percent_error2);
%fprintf("Water's thermal conductivity from reference is %0.4f W/mK at
%1.1f°C.\n",k_ref_WATER, Temperature_Fluid);

% IPA %
fprintf("Isopropyl alcohol's thermal conductivity at %1.1f°C is %0.4f W/mK
technique #1, percent error is %0.4f%%.\n",Temperature_Fluid, k1,
Percent_error1);
fprintf("Isopropyl alcohol's thermal conductivity at %1.1f°C is %0.4f W/mK
technique #2, percent error is %0.4f%%.\n",Temperature_Fluid, k2,
Percent_error2);
fprintf("Isopropyl alcohol's thermal conductivity from reference is %0.4f
W/mK at %1.1f°C.\n",k_ref_IPA, Temperature_Fluid);

% Ethanol %
% fprintf("Ethanol's thermal conductivity at %1.1f°C is %0.4f W/mK technique
#1, percent error is %0.4f%%.\n",Temperature_Fluid, k1, Percent_error1);
% fprintf("Ethanol's thermal conductivity at %1.1f°C is %0.4f W/mK technique
#2, percent error is %0.4f%%.\n",Temperature_Fluid, k2, Percent_error2);
% fprintf("Ethanol's thermal conductivity from reference is %0.4f W/mK at
%1.1f°C.\n",k_ref_Ethanol, Temperature_Fluid);

writematrix(THWM, 'THWM_IPA_45mA_gain5.csv');

```